

A novel enzymatic quantification method for polyphosphate in phytoplankton

By

Evelyn MacKay-Barr

A thesis submitted to the

Department of Chemistry and Biochemistry

Mount Allison University

in partial fulfillment of the requirements for the

Bachelor of Science degree

with Honours in Biochemistry

April 21, 2022

## Table of Contents

<b>Abstract</b> .....	<b>4</b>
<b>Acknowledgements</b> .....	<b>5</b>
<b>List of Abbreviations</b> .....	<b>6</b>
<b>List of Figures</b> .....	<b>8</b>
<b>Introduction</b> .....	<b>9</b>
<i>Phosphorus in the environment</i> .....	9
<i>The global phosphorus cycle</i> .....	9
<i>Phosphorus in biological systems</i> .....	11
<i>The structure and function of polyphosphate</i> .....	12
<i>Phytoplankton, polyphosphate, and the marine phosphorus cycle</i> .....	13
<i>The enzymes related to the construction and destruction of polyphosphate</i> .....	14
<i>Difficulties quantifying polyphosphate</i> .....	15
<i>Research objectives</i> .....	16
<b>Methods and Materials</b> .....	<b>17</b>
<i>Chemicals</i> .....	17
<i>Phytoplankton culturing and harvest</i> .....	17
<i>Transformation of scPpx1p and scIpp1p plasmids into bacterial expression cells</i> .....	18
<i>scPPX::pASG-IBA103 and scIPP::pASG-IBA105 transformed E. coli DH10<math>\beta</math> cell cultures</i> ..	18
<i>Plasmid purification and storage</i> .....	18
<i>Protein expression of scPPX::pASG-IBA103 and scIPP::pASG-IBA105</i> .....	18
<i>Electrotransformation of E. coli RIPL cells</i> .....	18
<i>Day cultures of transfected E. coli RIPL cells</i> .....	19
<i>Harvest and homogenization of E. coli RIPL cells</i> .....	19
<i>Protein purification</i> .....	19
<i>The column purification of scIpp1p and scPpx1p</i> .....	19
<i>Column regeneration</i> .....	20
<i>Protein concentration and SDS-PAGE analysis</i> .....	20
<i>Determination of specific activity of scIpp1p and scPpx1p</i> .....	21
<i>Ascorbate assay for polyphosphate quantification</i> .....	22
<i>Detection reagent preparation</i> .....	22

Polyphosphat analysis assay .....	22
<i>Polyphosphate extraction</i> .....	23
Christ and Blank extraction .....	23
Bru et al. extraction.....	23
<i>Phosphate quantification</i> .....	24
<i>Additional testing of assay ruggedness and robustness</i> .....	24
Interference of extraction and digestion materials on ascorbate assay response .....	24
Interference of extraction materials on scIpp1p and scPpx1p activity .....	24
<b>Results .....</b>	<b>25</b>
<i>Protein expression of scIpp1p and scPpx1p</i> .....	25
<i>Specific enzyme activity assays</i> .....	28
<i>Analysis of known polyphosphate amounts</i> .....	28
<i>Testing of ascorbate assay robustness and ruggedness</i> .....	31
<i>Optimized Christ and Blank polyphosphate extraction protocol trials</i> .....	33
<i>Bru et al. polyphosphate extraction protocol trial</i> .....	33
<b>Discussion.....</b>	<b>34</b>
<i>Expression and purification of scPpx1p and scIpp1p</i> .....	34
<i>Analysis of known polyphosphate amounts</i> .....	35
<i>Effects of extraction materials on assay response</i> .....	36
<i>Effects of extraction materials on enzyme activity</i> .....	37
<i>Polyphosphate in Polysiphonia</i> .....	37
<i>Troubleshooting the Christ and Blank extraction method</i> .....	37
<i>Polyphosphate in Synechocystis sp. PCC6803</i> .....	38
<i>Extraction of polyphosphate standards</i> .....	39
<b>Future Directions .....</b>	<b>40</b>
<b>Literature Cited .....</b>	<b>42</b>

## Abstract

Polyphosphate (polyP) is a basic biological polymer made up of linear chains of inorganic phosphate ( $P_i$ ) units linked by high-energy phosphoanhydride bonds. The presence of polyP is ubiquitous, but its study has historically been ignored and limited by difficulties in extracting and quantifying polyP from cells. Recently published analytical polyP extraction and enzymatic quantification methods claim to be the “gold standard” for quantitative polyP research but have not yet been tested in species other than *Saccharomyces cerevisiae*. The adaptation of these methods for use in the quantification of polyP in phytoplankton was attempted. The molybdenum blue assay, using cloned and expressed exopolyphosphatase (EC 3.6.1.11) and pyrophosphatase (EC 3.6.1.1) enzymes, very accurately determined the concentration of polyP in a sample after its enzymatic hydrolysis to  $P_i$ . Analyte response is largely unaffected by buffer contamination with phenol or chloroform and sample dilution with Milli-Q water. The polyP extraction methods were unsuccessful and not able to replicate the results of the published protocol when attempted on polyP standards or *Polysiphonia* samples. An older polyP extraction protocol was used to successfully extract polyP from *Synechocystis* sp. PCC6803 but was unable to extract polyP standards. By combining these older extraction methods and newly published enzymatic quantification methods, the concentration of polyP stored within the cells of phytoplankton and cyanobacteria can accurately be measured for future studies, but the cause of the inability of either method to extract polyP standards is still unknown.

## **Acknowledgements**

I would first like to thank Dr. Jeffrey Waller for acting as my supervisor throughout the year. His expertise and mentorship have allowed me to develop invaluable lab skills that I am certain will continue to serve me throughout my education and career beyond Mount Allison.

I would also like to thank Dr. Justin Liefer for acting as my supervisor throughout the year. His passion and support taught me to look at problems from multiple different angles and allowed me to progress without getting discouraged when I would run in to difficulties, instead turning them into learning opportunities.

I would also like to thank the members Team DMSP: Isaiah Baldwin, Shafkat Ahmed, and Maren Miller, for their support and presence in the lab and for making the research process so enjoyable over the summer.

Thank you to the entire Chemistry and Biochemistry and Biology departments at Mount Allison University, both the faculty and student body, for the pleasure I have had studying here these past four years.

I would also like to thank Dr. Jonas Christ and Dr. Lars Blank for providing the plasmids used to produce the enzymes necessary for this project, and for publishing the papers that inspired this work.

Finally, I would like to thank Petro Canada and Mount Allison University for funding this project and making this research possible.

### List of Abbreviations

$A_{260}/A_{280}$	Ratio of absorbance at 260 and 280 nm; used to assess DNA purity
$A_{882}$	Absorbance at 882 nm
AHTC	Anhydrotetracycline antibiotic
Amp	Ampicillin antibiotic
AMP	Adenosine monophosphate
AmpR	AmpR promoter; the promoter for ampicillin resistance in plasmids
ATP	Adenosine triphosphate
BG-11	Growth media optimized for cyanobacteria
BGG	Bovine $\gamma$ -globulin
BSA	Bovine serum albumin
C	Carbon
DMF	Dimethylformamide
DNA	Deoxyribonucleic acid
<i>E. coli</i>	<i>Escherichia coli</i>
EDTA	Ethylenediaminetetracetic acid
H	Hydrogen
hr	Hour
LB	Lysogeny broth
LN <sub>2</sub>	Liquid nitrogen
LSB	Laemmli sample buffer
min	Minute
MQ	Milli-Q water purified using a Milli-Q Water Purification System
N	Nitrogen

O	Oxygen
OD	Optical density
P	Phosphorus
PAGE	Polyacrylamide gel electrophoresis
pDNA	Plasmid deoxyribonucleic acid
P <sub>i</sub>	Phosphate or orthophosphate
polyP	Inorganic polyphosphate
polyP-12	Sodium hexametaphosphate; a polyP standard with a chain length of 12
polyP-45	Sodium polyphosphate standard with a chain length of 45
PP <sub>i</sub>	Inorganic pyrophosphate
RNA	Ribonucleic acid
scIpp1p	Inorganic pyrophosphatase from <i>S. cerevisiae</i>
scPpx1p	Exopolyphosphatase from <i>S. cerevisiae</i>
SDS	Sodium dodecyl sulfate
TC	Tetracycline antibiotic
TRIS	Tris(hydroxymethyl)aminomethane
U	Unit of enzyme activity where 1 μmol or pmol P <sub>i</sub> is released per min at 37°C
V	Volts
v/v	Volume/volume
w/v	Weight/volume
yr	Year

## List of Figures

Figure 1. The global phosphorus cycle .....	11
Figure 2. Chemical structure of polyphosphate .....	12
Figure 3. Enzymes involved in polyphosphate synthesis and utilization in prokaryotes .....	14
Figure 4. Acrylamide (10% w/v) gel electrophoresis analysis of scPpx1p fractions induced with 0.2 µg/mL UV-exposed tetracycline from column purification .....	26
Figure 5. Acrylamide (10% w/v) gel electrophoresis analysis of scIpp1p fractions induced with 0.2 µg/mL UV-exposed tetracycline from column purification .....	16
Figure 6. Acrylamide (10% w/v) gel electrophoresis analysis of scPpx1p fractions induced with 0.2 µg/mL anhydrotetracycline from column purification.....	27
Figure 7. Acrylamide (10% w/v) gel electrophoresis analysis of scIpp1p fractions induced with 0.2 µg/mL anhydrotetracycline from column purification .....	27
Figure 8. Standard curve of the ascorbate assay reaction with Na <sub>2</sub> PO <sub>4</sub> standards made with MQ water and extraction buffer at an absorbance of 882 nm .....	31
Figure 9. Ascorbate assay response to varying phosphate concentrations with varying buffer contamination levels and to constant Pi concentrations with varying buffer contamination at an absorbance of 882 nm .....	32
Figure 10. Enzymatic capacity of scIpp1p and scPpx1p to digest sodium hexametaphosphate spikes at differing levels of buffer contamination .....	33

## Introduction

### Phosphorus in the environment

Phosphorus (P) is an element essential to all life and is one of the main nutrients necessary for animal and plant growth. P can exist in multiple oxidation states, from -3 (as  $\text{PH}_3$  or  $\text{Ca}_3\text{P}_2$ ) to +5 (as  $\text{PO}_4^{3-}$ ), and only occurs naturally in combination with other elements (1, 2). P is most often found in compounds as groupings of phosphate minerals containing the tetrahedrally coordinated phosphate ( $\text{PO}_4^{3-}$ ) anion that fit into a crystal structure with other compounds, most commonly as the mineral apatite (3). Phosphate minerals used for agricultural fertilisers and many other industrial purposes are often mined from uplifted sedimentary layers that were previously deposited on the sea floor. The mineral deposition of phosphate occurs as it is precipitated from seawater and marine detritus, depositing on the sea floor to eventually become part of sedimentary rock (4, 5). Due to the critical role fertilizers play in contemporary agriculture the annual demand for P is growing rapidly, requiring more mining of these limited phosphate sediments (5). Some scientists believe that “peak phosphorus” (a concept describing the point where humanity will reach maximum global P production and use resulting in phosphate mineral shortages or price increases) might negatively affect worldwide food security and occur within the next 30 years (6). P itself is an abundant element in the Earth’s crust, with a concentration of about one gram per kilogram, but the richest deposits most easily accessible for mining are at risk of depletion (7). A large but mostly unavailable (to humans) pool of P is present in the Earth’s oceans. The marine P cycle regulates the availability of this nutrient to marine primary producers and thus limits ocean productivity, particularly over geological time, making it an integral part of global ocean function.

### The global phosphorus cycle

Unlike other macronutrient elements like carbon (C), sulfur, and nitrogen (N), the biogeochemical cycle of P has a relatively small atmospheric component, preventing the more frequent cyclic replenishment of soils seen in other macronutrient cycles (8). The global phosphorus cycle has four major components: the tectonic uplift of P-containing rocks, the erosion and weathering of P-containing rocks to produce soil and dissolved/particulate P in rivers, the riverine transport of P to lakes and ocean, and the sedimentation of organic and mineral P once in the ocean (Figure 1) (2). In the terrestrial portion of the P cycle, P resides in bedrock, soil, and the biomass of living organisms. The concentration of soil P is controlled by

its sorption to soil constituents like ferric iron and uptake by plants, which can produce chelating compounds, enzymes, or acids to solubilize bound P and  $P_i$  (9). Plants can minimize their P losses through the resorption of P prior to litterfall and the remineralization of P from detritus in the soil. Through erosion and weathering, P runoff enters rivers and is transported to the ocean. The amount of P discharge from rivers has been elevated due to human fertilizer use, increased deforestation and cultivation leading to increased erosion, and waste disposal, increasing global P delivery to surface waters from 5 Tg/yr in 1900 to 9 Tg/yr in 2000. In turn, this has resulted in the eutrophication of lakes and coastal areas and promoting harmful algal blooms and anoxic conditions in these waters (10). In the marine portion of the P cycle, P is linked to the marine C and N cycles through the assimilation of these elements by primary producers. This P is circulated in the ocean through the consumption and decomposition of P-containing organisms. The major pathway of P removal from the ocean is through the sinking organic matter to the seafloor and the subsequent sedimentation of P (2, 11).

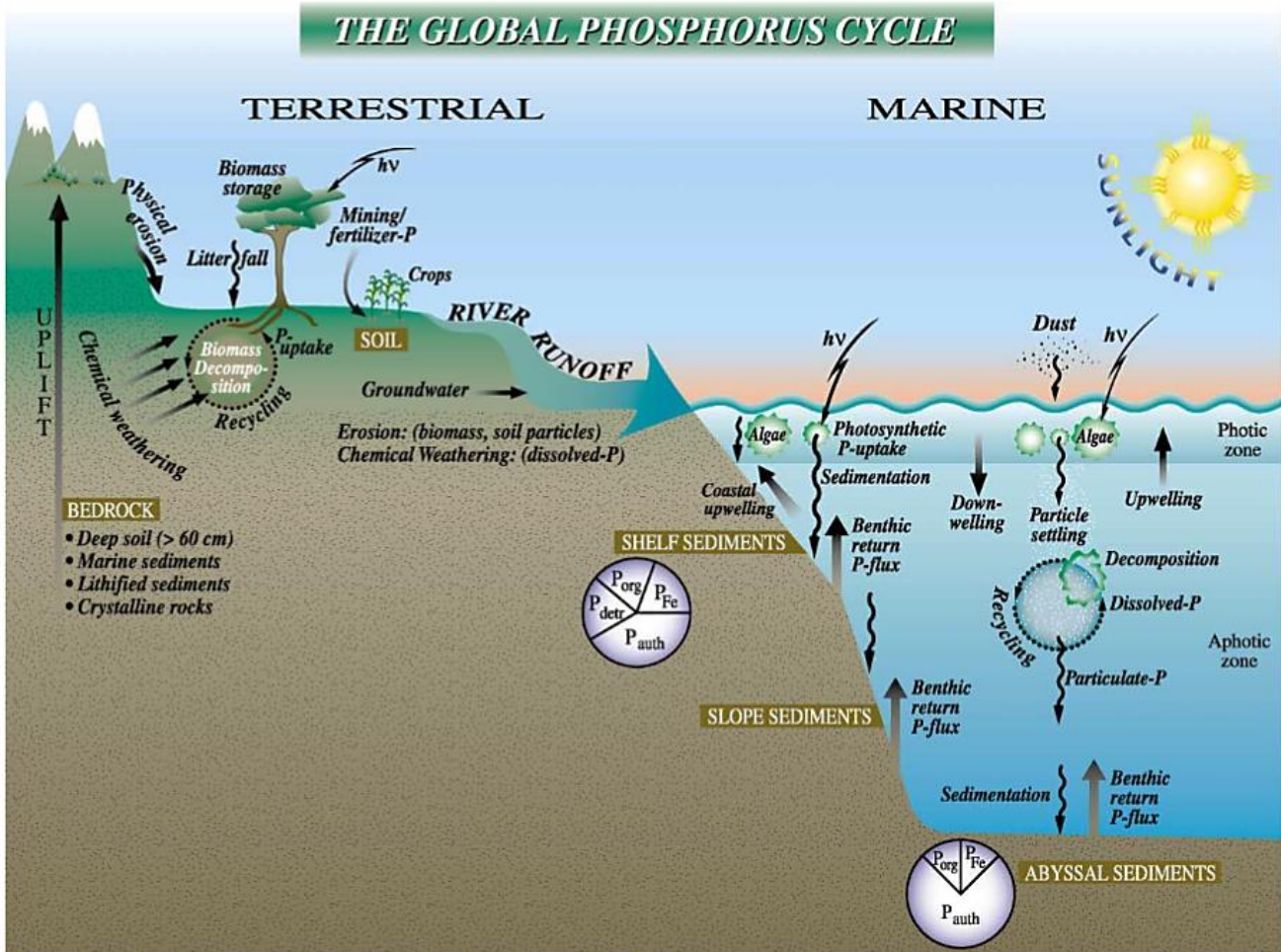


**Figure 1. The global phosphorus cycle.** The distribution of phosphorus (P) between different chemical and mineral forms in marine sediments is given in pie diagrams, where the abbreviations used are organic P (P<sub>org</sub>), iron-bound P (P<sub>Fe</sub>), detrital apatite (P<sub>detr</sub>), biogenic apatite (P<sub>auth</sub>). Image taken from Ruttenberg (2003) (2).

### Phosphorus in biological systems

P is an essential nutrient for all living organisms and makes up about 0.3% of the dry weight of living matter (12). Most P in biological systems is found in the fully oxidized form as compounds containing the PO<sub>4</sub><sup>3-</sup> ion (P<sub>i</sub>), typically either as free P<sub>i</sub>, complexed with Ca, or esterified to a carbon chain or another P<sub>i</sub> through a phosphoanhydride bond (13, 14). Important P-containing materials in biological systems are the P<sub>i</sub>-ester backbones of DNA and RNA, simple P<sub>i</sub>-esters like G6P and phospholipids, phosphorylated proteins, and phosphoanhydride bond-containing molecules ATP and ADP (15, 16). Through these structures, P<sub>i</sub> serves central biological functions in all living organisms, regulates enzyme function and cell signalling, and is the dominant energy currency, fueling most energy-requiring processes in the cell (17). Due to

the importance of this element, an organism may store P for later use when it is available in the environment. P availability often limits biological productivity in marine ecosystems, so this storage can be essential to organism survival (11, 12). This P can be stored as polyphosphate (polyP), the linear polymer of P<sub>i</sub> units linked by high-energy phosphoanhydride bonds, which can be found in all living organisms and can comprise over 60% of the total P in a cell (15, 18).

### The structure and function of polyphosphate

PolyP is the most simple biological polymer and can be tens or thousands of P<sub>i</sub> units long, with the smallest polyP being triphosphoric acid and consisting of three P<sub>i</sub> units (Figure 2) (19). PolyP is produced abiotically through the dehydration of phosphate rock at high temperatures and has been found in volcanic condensates and deep-ocean steam vents, making it a likely precursor to biotic evolution (14, 20). Its importance as an energy source to early life led to the evolution of polyP-producing enzymes (21). Despite polyP being a polymer found in every organism and existing since prebiotic times, the study of polyP has historically been neglected. It was considered an irrelevant ‘molecular fossil’ of energy distribution, replaced by the evolution of ATP (22). Recently, more efforts have been directed towards polyP as its physiological functions become known (23, 24).

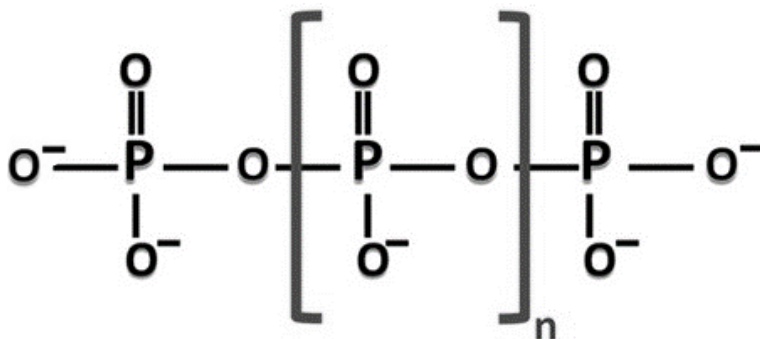


**Figure 2. Chemical structure of polyphosphate (polyP).** PolyP is a linear anionic polymer made up of at least two phosphate units linked by phosphoanhydride bonds.

While serving as a reservoir for P<sub>i</sub> and buffering changes in cellular P<sub>i</sub>, polyP is also used to phosphorylate nucleotide mono- and diphosphates to produce energy molecules like ATP and GTP (22). PolyP is anionic in nature, enabling it to bind and sequester cations. This can contribute to the heavy metal tolerance of cells through the chelation of metal ions, allow polyP to act as components in membrane ion channels, as molecular chaperones, and as a sequestration site for elevated intracellular cation concentrations (24–26). These roles allow polyP to aid in an

organism's acclimation to biotic and abiotic stresses, including nutrient deprivation (20). PolyP is also involved in cellular processes like apoptosis, cellular signalling, biofilm formation, and sporulation. In organisms with defects in polyP synthesis, abnormalities and the inability to perform in these areas have been exhibited (24).

### **Phytoplankton, polyphosphate, and the marine phosphorus cycle**

Since phytoplankton are the primary producers that support most marine food webs, they take up and fix C, N, and P and make them available for other organisms and biogeochemical cycling. The elemental stoichiometry (C:N:P) of phytoplankton is assumed to follow the Redfield ratio (106:16:1) but the C:N:P of phytoplankton can vary greatly. Since P is a limiting nutrient to cell growth in many parts of the ocean, the C:N:P of phytoplankton is often dependent on P availability, which influences macronutrient use by consumers, biogeochemical cycles, and the export of biomass to the deep ocean in turn (27). Phytoplankton primary production and its export to the deep ocean are the primary method in which the ocean sequesters C over geological time, making P availability and use a critical component in global C storage and changes to the Earth's climate (11). It is also estimated that phytoplankton produce about 70% of the atmospheric oxygen on the planet, making them very important organisms not only in ocean ecology, but to all land organisms as well (28). This makes knowing the amount of P available in cells and in the ocean in general integral to modeling photosynthesis and C sequestration for research on climate change.

Despite the importance of P availability being well known, how it is allocated within the cell is poorly understood. The P-containing molecules within cells are known but the amount of each of these present in a cell can change between species or in different conditions. The recycling of P located in phospholipids and RNA in phytoplankton experiencing P stress has been documented, but phytoplankton appear to retain high levels of polyP even when P is extremely scarce (29). This indicates its importance not only as a P storage molecule but in regulatory roles within the cell. PolyP is thought to represent one of the largest fractions of P in phytoplankton and the ocean itself, although the true portion of total P that polyP makes up is not known, making it a critical component of the global P cycle (22, 29).

## The enzymes related to the construction and destruction of polyphosphate

The only prokaryotic polyP synthetic enzyme with homologues in eukaryotes is polyphosphate kinase 1 (EC 2.7.4.1); encoded by *ppk1* (30). PolyP kinases are enzymes that reversibly add a phosphate group to the end of a polyP chain by transferring energy-rich  $P_i$  residues from ATP to polyP or from polyP to ADP (31, 32). It is the main enzyme for polyP synthesis as it is the only enzyme that preferentially catalyzes the  $\text{polyP}_n \rightarrow \text{polyP}_{n+1}$  reaction. Polyphosphate kinase 2 (EC 2.7.4.34), encoded by *ppk2*, differs from polyP kinase 1 in that it uses polyP in the reversible generation of GTP; polyphosphate-AMP phosphotransferase (EC 2.7.4.33) phosphorylates AMP to ADP using polyP (33). The reactions catalyzed by these enzymes, although reversible, have preferences for the degradation of polyP (30). Fewer polyP synthesizing enzymes have been identified in eukaryotes than in prokaryotes; polyP chains in eukaryotes are synthesized by the vacuolar transporter chaperone complex (34).

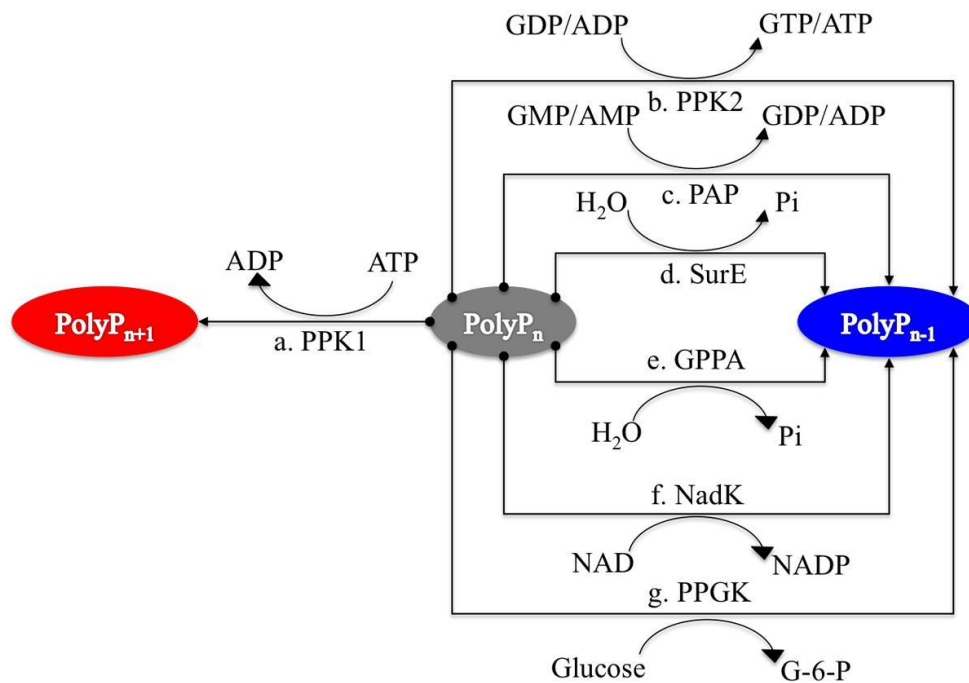


**Figure 3. Enzymes involved in polyphosphate (polyP) synthesis and utilization in prokaryotes.** PolyP kinase 1 (PPK1) represents the synthesis enzyme for polyP while polyP kinase 2 (PPK2), polyP-AMP-phosphotransferase (PAP), 5'/3'-nucleotidase (SurE), guanosine pentaphosphate phosphohydrolase/exopolyPase (GPPA), NAD kinase (NadK), polyP glucokinase (PPGK) are biased towards polyP degradation despite being reversible reactions. Schematic from Wang *et al.* (2018) (30).

Some of the most important enzymes for polyP catabolism are the polyphosphatases, which exist in both prokaryotes and eukaryotes (30, 35). There are several types of polyphosphatases, mainly exopolyphosphatases (EC 3.6.1.11), which break the phosphoanhydride bonds of polyP through hydrolysis and cleave  $P_i$  from the end of polyP chains until only inorganic pyrophosphate ( $PP_i$ ) remains (35). There are also endopolyphosphatases (EC 3.6.1.10) that cleave internal phosphoanhydride bonds, cutting long polyP chains into shorter ones (33) (Figure 3). Exopolyphosphatases are useful when trying to enzymatically quantify polyP due to its substrate specificity for polyP of different chain lengths but not molecules like ATP and other nucleoside triphosphates or  $PP_i$  (32).

### **Difficulties quantifying polyphosphate**

While polyP is increasingly becoming the focus of microbiological and environmental study, the understanding of the significance and roles of polyP is hindered by the lack of easy quantitative methods (36). Common analytical approaches like  $^{31}P$  NMR spectroscopy require large sample sizes that are difficult to collect from filtered ocean water, may be insensitive to polyP associated with metal cations in solid granules, and cannot distinguish between polyP and other phosphoanhydride bond-containing molecules (37, 38). Raman spectroscopy can also be used to quantify and localized polyP in algae, but these methods are expensive, difficult, and have low throughput compared to others available (39). Fluorescence-based polyP analysis methods are not quantitative due to the fluorescent response differing between polyP standards and natural polyP and are non-specific, being subject to interference by other  $P_i$ -containing compounds within the cell (36, 37). To avoid interference by these compounds, polyP can be differentially extracted from the cell and precipitated. Other polyP quantification methods use these purification techniques, but they are cumbersome, non-specific if contaminating  $P_i$ -containing molecules remain, and likely damage and miss some of the polyP within the cell (37). Assays using enzymes of polyP metabolism followed by colorimetric  $P_i$  determination involve the purification of extracted polyP, which results in lowered analyte measurements as some will remain with the removed contaminants or in the vessel used. Enzymatic polyP quantification methods also require enzymes with a high specificity for polyP and the ability to fully digest polyP to  $P_i$ , as exopolyphosphatases leave  $PP_i$  behind after hydrolysis, lowering total polyP measurement (36).

The lack of truly quantitative and available methods for polyP analysis has limited research in the past, but analytical methods for polyP extraction and quantification that are unhindered by the listed difficulties are being developed (38, 40). An established extraction method for polyP, referred to as the Bru *et al.* protocol, involved using buffers, detergents, phenol, and heat to extract polyP from cells, then chloroform to partition and remove phenol and non-polar contaminants in the extract. The collected aqueous phase is then treated with nucleases to destroy the P-rich RNA and DNA that could act as sources of  $P_i$ , then ethanol to precipitate and purify the extracted polyP (38). These methods take 5.5 hr to complete and some polyP is likely lost during the purification steps. Optimized methods for analytical polyP extraction based on the Bru *et al.* protocol have recently been published by Jonas Christ and Lars Blank of Aachen University in Germany. Developed for use on *Saccharomyces cerevisiae*, these optimized methods require only 30 min and eliminate the use of detergents, nucleases, and need for polyP purification, reporting yields of 40% more polyP than the original Bru *et al.* protocol (38, 40). Christ and Blank have also developed an enzymatic assay where polyP is hydrolyzed to  $P_i$  using exopolyphosphatase 1 from *S. cerevisiae* (scPpx1p) and inorganic pyrophosphatase (EC 3.6.1.1) from *S. cerevisiae* (scIpp1p), enzymes that only target polyP and  $PP_i$  and not contaminating molecules like ATP or DNA. Released  $P_i$  is measured using an optimized one-reagent colorimetric  $P_i$  assay that forms the pigment molybdenum blue, resulting in both polyP quantity and chain length measurement (41). They propose their method as the new gold standard for analytical polyP extraction and quantification from *S. cerevisiae*. Although the method is species-independent, it has only been tested on *S. cerevisiae* and not yet been applied to any other organisms like phytoplankton (40). They have also not verified their polyP extractions and measurements using spike and recovery tests with polyP standards or examining total P content in the cell to ensure their results, with the P from other pools, summed to total cellular P. Without tests like these to confirm the results of their extraction method, it cannot yet be accepted as the gold standard of polyP extraction.

### **Research objectives**

This research project aimed to confirm that the polyP extraction and quantification methods designed by Christ and Blank are both robust and rugged, and that they can be used to determine the amount of  $P_i$  stored in the form of polyP chains in laboratory cultures of different phytoplankton species. It was hypothesized that large, variable P storage pools exist in

phytoplankton as polyP and represent a large amount of residual P that has been difficult to quantify due to methodological challenges (31). To quantify these polyP stores, the newly developed enzymatic method for analyzing polyP in yeast developed by Christ and Blank was adapted for use in phytoplankton (40, 41). To do this, *scIpp1p* and *scPpx1p* in protein expression vectors were obtained, expressed in a bacterial host, and purified. The activity of *scIpp1p* and *scPpx1p* was determined and the enzymes were used to analyze polyP extracted from phytoplankton samples. This method could overcome the methodological challenges preventing the quantification of polyP in phytoplankton and other globally significant organisms. Accurate polyP measurements will address the limited knowledge of how phytoplankton utilize  $P_i$  within their cells and how it affects their growth and will also strengthen efforts to model the marine P cycle and its role in the global ocean ecology.

## Methods and Materials

### Chemicals

All chemicals were purchased from BioShop Canada, Sigma-Aldrich, New England Biolabs, Fisher Scientific, or BioRad. Buffers were prepared using ultrapure water purified using a Milli-Q Reference Plus system (MQ), adjusted to target pH levels, and stored at 4°C or -20°C.

### Algal culturing and harvest

The red macroalgae *Polysiphonia lanosa* was collected from Mispec Beach, NB in August 2019, where it was found growing on another algal species. Samples were drained, snap frozen in liquid nitrogen ( $LN_2$ ), and stored at -80°C until use. *Polysiphonia* samples were taken from storage and lyophilized for roughly 24 hr, before being measured out into 1.4-2.1 mg aliquots in bead-filled tubes for polyP analysis. All *Polysiphonia* aliquots were stored at -80°C until tested.

The cyanobacterium *Synechocystis* sp. PCC6803 was grown in BG-11 media under an irradiance of about 80  $\mu\text{mol photons m}^{-2} \text{ s}^{-1}$  with a 12:12 hr light-dark cycle. Cultures were constantly agitated on a shaker to prevent cells from clumping together. Culture samples were transferred to Falcon tubes and centrifuged to collect cells at the bottom of the tube before media was poured off and cells were transferred to reaction tubes for extraction.

## **Transformation of scPpx1p and scIpp1p plasmids into bacterial expression cells**

Construct plasmid DNA (pDNA) was provided by Jonas Christ, encoding the genes *scPPX::pASG-IBA103* and *scIPP::pASG-IBA105* from *S. cerevisiae* VH2.200 (industrial baker's yeast strain) with Twin-Strep-tag affinity tags on the C- (for scPpx1p) and N-termini (for scIpp1p) of the recombinant proteins. Provided pDNA was electroporated into *Escherichia coli* DH10 $\beta$  cells using a BioRad MicroPulser on Ec1 with time constants of 5.50 ms. The cells were recovered in lysogeny broth (LB, 1% w/v tryptone, 0.5% w/v yeast extract, 1% w/v NaCl, pH 7.0) and incubated at 37°C with shaking at 200 rpm for 1 hr. Afterwards, cells were spread on AmpR selective LB-agar plates containing 50  $\mu$ g/mL ampicillin (Amp) and incubated at 37°C overnight.

### ***scPPX::pASG-IBA103* and *scIPP::pASG-IBA105* transformed *E. coli* DH10 $\beta$ cell cultures**

Two LB broth cultures with 50  $\mu$ g/mL Amp were inoculated from LB-agar plate *E. coli* DH10 $\beta$  colonies, one with *scPPX::pASG-IBA103* and the other with *scIPP::pASG-IBA105* transformed *E. coli*, and incubated overnight at 37°C, 200 rpm, at a 45° incline.

### **Plasmid purification and storage**

The purification of the *scPPX::pASG-IBA103* and *scIPP::pASG-IBA105* plasmids from overnight *E. coli* DH10 $\beta$  broth cultures was performed according to the Monarch Plasmid Miniprep Kit (#T1010) (New England BioLabs, Ipswich MA, USA). The pDNA was eluted with MQ water. The sample's purity was assessed through the  $A_{260}/A_{280}$  ratio of the DNA as measured with a NanoDrop 1000 spectrophotometer (Thermo Scientific, Waltham MA, USA), where a pure sample was considered to have a ratio greater than 1.8. Bacterial glycerol stocks containing the isolated pDNA were made by mixing equal parts glycerol and LB broth then were frozen in LN<sub>2</sub> and stored at -80°C to preserve the scPpx1p and scIpp1p pDNA-harboring cells. Pure pDNA was snap frozen in LN<sub>2</sub> and stored at -20°C.

### **Protein expression of *scPPX::pASG-IBA103* and *scIPP::pASG-IBA105***

#### *Electrotransformation of E. coli RIPL cells*

*scPPX::pASG-IBA103* and *scIPP::pASG-IBA105* pDNA were transformed into electrocompetent *E. coli* BL21 CodonPlus (DE3) RIPL cells (RIPL) for increased protein expression. The time constant of electroporation was 5.20 ms for *scPPX::pASG-IBA103* and 5.60 ms for *scIPP::pASG-IBA105*. Cells were recovered in LB media with 50  $\mu$ g/mL Amp and

incubated at 37°C with agitation at 200 rpm for an hour. Cells were plated onto LB agar plates containing 1% (w/v) glucose and 50 µg/mL Amp and incubated overnight at 37°C. Overnight broth cultures (LB, 50 µg/mL Amp) were made from the electrotransformed RIPL cells.

#### *Day cultures of transfected E. coli RIPL cells*

Day cultures of RIPL cells transformed with *scPPX::pASG-IBA103* and *scIPP::pASG-IBA105* were prepared using the overnight cultures with inoculum quantified by measuring optical densities at 600 nm (OD<sub>600</sub>) with a Molecular Devices SpectraMax M3 spectrophotometer and Softmax Pro program. The volume necessary to inoculate a day culture to an OD<sub>600</sub> of 0.05 was calculated from this. Day cultures were prepared with 400 mL LB broth (50 µg/mL Amp) and incubated at 37°C at 200 rpm until reaching an OD<sub>600</sub> between 0.5-0.8. Protein expression was induced with anhydrotetracycline (0.2 µg/mL AHTC) dissolved in dimethylformamide (DMF). Incubation continued at 30°C and 200 rpm for 3 hours.

There was no AHTC available during the first protein expression trial so tetracycline (TC) (2 mg/mL in DMF) was exposed to direct sunlight for 20 min and UV light for 15 min in an attempt to induce TC photolysis to produce AHTC before inducing protein expression (42).

#### *Harvest and homogenization of E. coli RIPL cells*

Day cultures were transferred to clean centrifuge bottles and centrifuged (12 min, 4500 rcf, 4°C). Supernatant was discarded and pellets were resuspended and pooled in 10% (v/v) glycerol before centrifugation (12 min, 4500 rcf, 4°C), supernatant removal, freezing of the cells in LN<sub>2</sub>, and storage at -80°C. All proceeding steps were carried out on ice. Cells pellets were resuspended in 10 mL buffer W (100 mM TRIS-HCl (pH 8.0), 150 mM NaCl, 1 mM EDTA). Cells were homogenized using an Avestin Emulsiflex B-15 homogenizer at 21 000 psi, passing through it three times. Insoluble cell debris was removed via centrifugation (15 min, 16 000 rcf, 4°C). Lysate and cell debris were frozen separately in LN<sub>2</sub> and kept at -80°C until protein purification.

### **Protein purification**

#### *The column purification of scIpp1p and scPpx1p*

The lysate was centrifuged again prior to purification (5 min, 16 900 rcf, 4°C). Two 1 mL Strep-Tactin XT Superflow columns (IBA Lifesciences, Göttingen, Germany) were washed with 5 mL buffer W to equilibrate them. The cell lysate was applied to the columns and washed with 7 mL buffer W, which was collected as the 'wash' fraction. Enzymes were eluted with ten 0.5

mL buffer BXT (buffer W saturated with biotin) volumes and eluate was collected in ten 0.5 mL fractions. Enzyme eluates were diluted 1:1 with glycerol, frozen with LN<sub>2</sub>, and stored at -80°C. Buffer BXT was prepared by dissolving biotin in hot buffer W (with the addition of NaOH to speed up dissolution) to a concentration of 50 mM, storing at 4°C overnight, and filtering through 0.2 µm pores to remove precipitate.

#### *Column regeneration*

The columns were regenerated with 15 mL 3 M MgCl<sub>2</sub> solution (filtered through 0.2 µm pores) to remove the biotin that eluted the protein extracts. 8 mL buffer W was applied to each column to remove the MgCl<sub>2</sub> and columns were stored at 4°C in buffer W until their next use.

#### **Protein concentration and SDS-PAGE analysis**

Using an enhanced Bradford protein assay, the soluble protein content of the cell lysate, the 'wash' fraction, and each enzyme eluate was quantified (43, 44). A bovine γ-globulin (BGG) standard curve ranging from 0.0-10.0 µg was used to quantify all measurements. BioRad Bradford protein dye reagent was diluted to working strength with MQ water and protein standards and soluble fractions were treated with 250 µL of the dye before a ten-minute incubation at room temperature and absorbance measurements at 590 and 450 nm using a Molecular Devices SpectraMax M3 spectrophotometer. The A<sub>590</sub>/A<sub>450</sub> ratio was used to quantify protein concentration.

The insoluble fraction was analyzed by mixing a portion of it with 400 µL 4X Laemmli sample buffer (LSB), submerging it in boiling water for 5 min, cooling it to room temperature, and centrifuging it (2 min, 10 000 rcf). The insoluble fraction's protein concentration was quantified by pipetting 1 µL of the LSB-solubilized fraction at 1:1, 1:2, and 1:4 dilutions (diluted with 4X LSB) onto chromatography paper along with bovine serum albumin (BSA) standards at concentrations ranging from 0.05-10.0 mg/mL. The dried paper was stained with Coomassie Brilliant Blue Stain (1% w/v Coomassie R-250 Brilliant Blue, 10% v/v acetic acid, 50% methanol, 40% MQ water) for 1 hr with agitation and destained with destain solution and agitation (10% v/v acetic acid, 40% v/v MQ water, 50% v/v methanol).

The soluble, insoluble, and purified fractions were then resolved on a 10% (w/v) polyacrylamide gel at 200 V until the dye front ran off the gels with SDS running buffer (2.5 mM TRIS, 9.2 mM glycine, 0.1% w/v sodium dodecyl sulfate (SDS)), 10 µg protein per well, and using an MBI Rainbow Pre-stained protein ladder (Cat. No. MRPPEVL). Protein samples

were prepared with 1X LSB, submerged in boiling water for 5 min, and centrifuged (2 min, 10 000 rcf) before being added to the wells of the gel. The gels were stained with agitation over three days and destained in a similar manner to the chromatography paper for comparison of protein content and purity.

### **Determination of specific activity of scIpp1p and scPpx1p**

The specific activity of scIpp1p was measured by preparing three microreaction tubes, tube 1 with 166  $\mu\text{L}$  scIpp1p buffer (300 mM TRIS-HCl, 6 mM  $\text{MgCl}_2$ , pH 7.2), 166  $\mu\text{L}$   $\text{P}_i$  (6 mM), 166  $\mu\text{L}$  MQ water, and 1  $\mu\text{L}$  scIpp1p (33 ng/ $\mu\text{L}$  scIpp1p in enzyme storage buffer), tube 2 being identical to tube 1 but without the enzyme, and tube 3 with 166  $\mu\text{L}$  scIpp1p buffer and 334  $\mu\text{L}$  MQ water. All tubes were incubated for 10 min at 25°C, then tube 1 was diluted 1:10 in MQ water and tubes 2 and 3 were diluted 1:10 in 111  $\mu\text{M}$   $\text{P}_i$ . 100  $\mu\text{L}$  from each was transferred to a 96-well plate, 50  $\mu\text{L}$  enzyme reaction buffer (60 mM TRIS-HCl (pH 7.5) 15 mM magnesium acetate, 150 mM ammonium acetate, filtered through 0.2  $\mu\text{m}$  pores) and 50  $\mu\text{L}$   $\text{P}_i$  detection reagent (solution B) were added and absorbance at 882 nm ( $A_{882}$ ) was measured after two min at room temperature. Specific activity of scIpp1p was calculated according to the following equation:

$$\text{specific activity}_{scIpp1p} \left[ \frac{U}{mg} \right] = \frac{(\text{Tube 1} - \text{Tube 2} + \text{Tube 3} [\mu\text{M } \text{P}_i]) \times 500}{\text{Mass scIpp1p} [ng]}$$

Sodium hexametaphosphate, a polyP standard with a chain length of 12 (polyP-12), obtained from Sigma-Aldrich (#305553) was used as a high purity polyP standard to test enzyme activity. The specific activity of scPpx1p was measured in a 96-well plate where well 1 contained 100  $\mu\text{L}$  polyP-12 (equivalent to 150  $\mu\text{M}$   $\text{P}_i$  after hydrolysis), well 2 contained 50  $\mu\text{L}$  polyP-12 (300  $\mu\text{M}$   $\text{P}_i$ ) and 50  $\mu\text{L}$   $\text{P}_i$  (200  $\mu\text{M}$ ), and well 3 contained 50  $\mu\text{L}$  MQ water and 50  $\mu\text{L}$   $\text{P}_i$  (200  $\mu\text{M}$ ). Afterwards, 50  $\mu\text{L}$  enzyme reaction buffer was added to each well and 1  $\mu\text{L}$  scPpx1p (1.5 ng/ $\mu\text{L}$  scPpx1p in enzyme storage buffer) was added to well 1 before incubating the plate at 37°C for 10 min. 50  $\mu\text{L}$  solution B was added to each well and  $A_{882}$  was measured after two min at room temperature. Specific activity of scPpx1p was calculated according to the following equation:

$$\text{specific activity}_{scPpx1p} \left[ \frac{U}{mg} \right] = \frac{(\text{Well 1} - \text{Well 2} + \text{Well 3} [\mu\text{M } \text{P}_i]) \times 10^7}{\text{Mass scPpx1p} [ng]}$$

Following the specific activity determination of scIpp1p and scPpx1p and the protein concentrations measured by the Super Bradford assay, the enzyme solutions were diluted to a target concentration of  $1.1 \times 10^4$  U scPpx1p/ $\mu$ L and  $1.3 \times 10^{-2}$  U scIpp1p/ $\mu$ L with enzyme storage buffer (20 mM TRIS-HCl (pH 7.5) 50% v/v glycerol, 50 mM KCl, filtered through 0.2  $\mu$ m pores, stored at  $-20^\circ\text{C}$ ). Diluted enzyme solutions were aliquoted in microtubes to reduce the thawing and freezing of enzymes between assays, frozen in LN<sub>2</sub>, and stored at  $-80^\circ\text{C}$  until use.

### **Molybdenum blue assay for polyphosphate quantification**

#### *Detection reagent preparation*

Solution A (2.4 mM ammonium heptamolybdate (Sigma #09878), 600 mM H<sub>2</sub>SO<sub>4</sub> (Sigma #258105), 0.6 mM antimony potassium tartrate (Sigma #383376)) was prepared by first dissolving antimony in MQ water, adding H<sub>2</sub>SO<sub>4</sub>, then dissolving the molybdate. This solution was stored at  $4^\circ\text{C}$  in a bottle protected from light for up to a month. Solution B was prepared by dissolving ascorbic acid (Fisher #BP351) up to 88 mM in solution A and was prepared fresh immediately prior to use.

#### *Polyphosphate analysis assay*

The polyP sample being analyzed (either a known amount of polyP standard or an extracted sample with unknown polyP content) was diluted with MQ water to yield approximately 180  $\mu$ M total P<sub>i</sub> once polyP is digested. The assays were conducted according to the methods outlined by Christ and Blank, with the alteration that, besides blanks, all samples were treated with both scPpx1p and scIpp1p as the chain length of polyP was not of particular interest (41). The diluted sample (100  $\mu$ L) was added to a 96-well microplate and 50  $\mu$ L of enzyme reaction buffer was added, with 1  $\mu$ L of diluted scIpp1p and 1  $\mu$ L of diluted scPpx1p added to each digestion sample. The 96-well microplate being used was covered with Parafilm M tape to avoid evaporation and placed in a hot air incubator set to  $37^\circ\text{C}$  for an hour. After incubation, 50  $\mu$ L of solution B was added to each well and after 2 min at room temperature A<sub>882</sub> was measured using a Molecular Devices M3 spectrophotometer and the Softmax Pro program. Every sample, both those treated with scPpx1p and scIpp1p and those treated with neither to act as a P<sub>i</sub> blank, was run in triplicate.

## **Polyphosphate extraction**

### *Christ and Blank extraction*

The first extraction process used followed that outlined by Christ and Blank (40). Between 1-2 mg of cell biomass or a known amount of polyP-12 (a polyP standard with a chain length of 12 P<sub>i</sub> units) was added to 2 mL bead tubes (MP Biomedicals, Lysing Matrix D) or 1.7 mL reaction tubes and ME-buffer (25 mM MOPS (pH 7.0), 2.5 mM EDTA, filtered through 0.2 µm pores, stored at 4°C) was added before vortexing. Phenol (Bioshop #PHE510) was buffered with a provided TRIS buffer to achieve a pH of 7.9 as per manufacturer instructions and was added to the tube before vortexing and incubating for 10 min at 45°C in a heating block followed by 2 min on ice. When bead tubes were used a bead milling step (2x30 s, 6.5 m/s, 1 min rest on ice between) was added between the addition of phenol and incubation at 45°C. Chloroform (Sigma, HPCL-grade) was added to extract phenol dissolved in the aqueous phase and the tube was vortexed before low-density phase lock gel (autoclaved high vacuum grease) was applied inside the lid of the tube before centrifugation (5 min, 12 000 rcf) (40). The top aqueous phase was then transferred to another tube and the exact volume extracted was noted. This polyP extract was used for enzymatic polyP analysis.

### *Bru et al. extraction*

The second extraction process followed the process outlined by Bru *et al.* (38). All volumes used were increased by 50%. A cell biomass of about 2.0 mg or a known amount of sodium polyphosphate (Sigma #S4379) with a chain length of 45 P<sub>i</sub> units (polyP-45) was transferred to 1.7 mL reaction tubes and frozen to -20°C to break the cell walls and membranes. Samples were resuspended in 300 µL of AE-buffer (50 mM sodium acetate (pH 5.3), 10 mM EDTA) per 1 mg of cell mass. Phenol and 10% (w/v) SDS were added to the tube and contents were mixed by inverting and vortexing, incubated at 65°C for 5 min, and chilled for 1 min on ice. Chloroform was added and the tube was inverted, vortexed, and centrifuged (2 min, 13 000 rcf). The aqueous phase containing polyP was transferred to a tube containing chloroform, mixed by inverting and vortexing, and centrifuged (2 min, 13 000 rcf). The aqueous phase was transferred to a new tube and 3 µL of 10 mg/mL RNase A and 4 µL of 5 mg/mL DNase I were added per 600 µL of aqueous phase before incubating at 37°C for 1 hr. Contents were transferred to two tubes containing absolute ethanol and 3 M sodium acetate (pH 5.3) pre-chilled to -20°C. Tubes were kept at -20°C overnight to precipitate the polyP until centrifugation (20 min, 13 000 rcf,

4°C). The supernatant was discarded, the tubes were centrifuged (1 min, 13 000 rcf), and remaining ethanol was removed by pipetting. The tubes were left open in a sterile biosafety cabinet to dry remaining ethanol, and the polyP pellets were resuspended in MQ water prior to enzymatic polyP analysis.

### **Phosphate quantification**

The conversion of measured  $A_{882}$  to  $P_i$  concentration was conducted using a calibration curve of  $Na_2PO_4$  standards (0, 20, 65, 110, 155, and 200  $\mu M P_i$ ) dissolved in MQ water during the ascorbate acid-based polyphosphate analysis assay. Standards were run in duplicates and treated like regular samples.

### **Additional testing of assay ruggedness and robustness**

#### *Interference of extraction and digestion materials on ascorbate assay response*

The interference effects of buffer contamination with extraction and digestion materials on  $P_i$  quantification were measured by preparing  $Na_2PO_4$  standards identical to those used in the standard curve but dissolved in extraction buffer (blank top phase from the extraction process) and enzyme buffer (scIpp1p and scPpx1p in enzyme storage buffer). The resulting slope was compared to the standard curve slope to examine varying  $P_i$  concentration at a constant, maximal contamination level. The effects of varying  $P_i$  concentration with varying contaminant concentrations on assay response were examined by spiking extraction buffer with  $P_i$  and putting it through the digestion process. Afterwards, the spiked samples were diluted to various amounts (1:2 to 1:10) with MQ water in the 96-well microplate immediately before the addition of solution B. The response of a constant  $P_i$  concentration with varying buffer contamination was examined by running blank extraction buffer through the digestion and incubation process then diluting these blanks (1:2 to 1:15) and spiking each dilution with a constant amount of  $P_i$  before the addition of solution B.

#### *Interference of extraction materials on scIpp1p and scPpx1p activity*

To test the effects of buffer contamination on enzyme activity, extraction blanks were diluted 1:2, 1:4, and 1:8 with MQ water and spiked with a constant amount of polyP-12 before digestion and incubation. Since the concentrations of polyP-12 and enzymes added were constant, a comparison of colour development and  $A_{882}$  between dilutions allowed the

identification of a minimum dilution level necessary for enzymatic polyP digestion to run to completion.

## Results

### Protein expression of scIpp1p and scPpx1p

The first protein expression trial performed with the *scIPP::pASG-IBA105* and *scPPX::pASG-IBA103* constructs in *E. coli* cells was induced using the UV-exposed TC. After protein expression and cell harvest and lysis, Strep-Tactin XT Superflow columns were used to purify the expressed scIpp1p and scPpx1p, which had Twin-Strep-tag affinity tags on their N- and C-termini, respectively. The protein content from each stage of purification was compared using SDS-PAGE analysis. The expressed scPpx1p was clearly found to be its expected size of 45 kDa (Figure 4) and scIpp1p was found to be its expected size of 32 kDa, though the stained protein was faint (Figure 5). The purification was seen to be effective as contaminating protein bands became less abundant as the purification stages progressed, however, contaminating proteins were still found in the purified elution fractions.

The enzymes scPpx1p and scIpp1p were expressed and purified thrice more afterwards, induced using AHTC these times instead of the UV-exposed TC. The clarity of the expressed scPpx1p bands were variable depending on the expression, with some dark contaminating protein bands (Figure 6). The expressed scIpp1p bands were very clear this time, with some faint contaminating protein bands still present (Figure 7). Some of the contaminating protein bands were able to be identified as both scIpp1p and scPpx1p in the elution fractions in which they were not expressed, indicating that these expression trials were contaminated with each other.

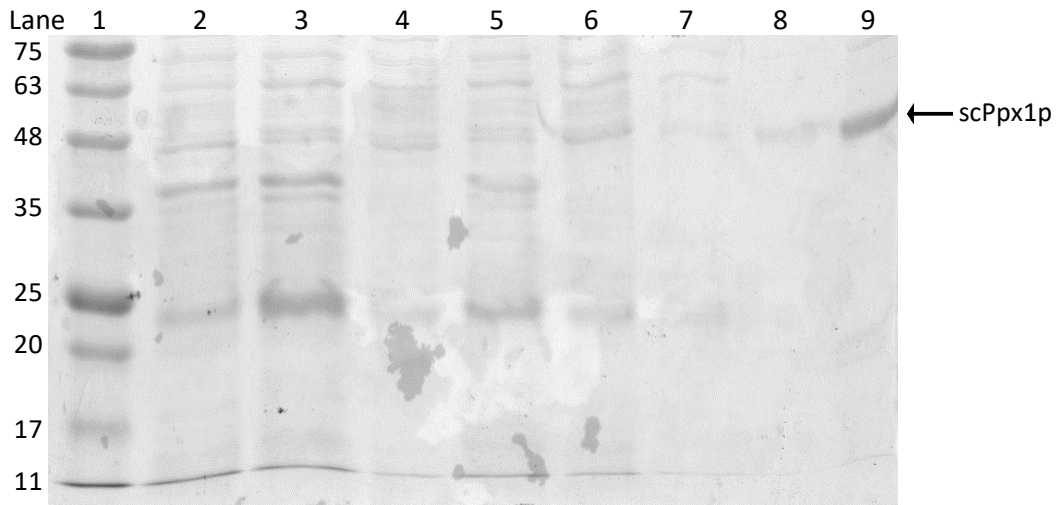


**Figure 4. Acrylamide (10% w/v) gel electrophoresis analysis of scPpx1p fractions induced with 0.2 µg/mL UV-exposed tetracycline from column purification.** scPpx1p was expressed in *E. coli* RIPL cells. The soluble fraction was passed through a 1 mL Strep-Tactin XT Superflow column and eluted with BXT buffer. Protein was stained using Coomassie Brilliant Blue R-250. Lane 1: MBI Rainbow Prestained Protein Evolution Ladder; lane 2: pre-induction cell pellet (10 µg); lane 3: post-induction cell pellet (10 µg); lane 4: soluble fraction (10 µg); lane 5: insoluble fraction (10 µg); lane 6: non-binding eluate (10 µg); lane 7: wash (10 µg), lane 8: elution fraction (2 µg); lane 9: elution fraction (10 µg).

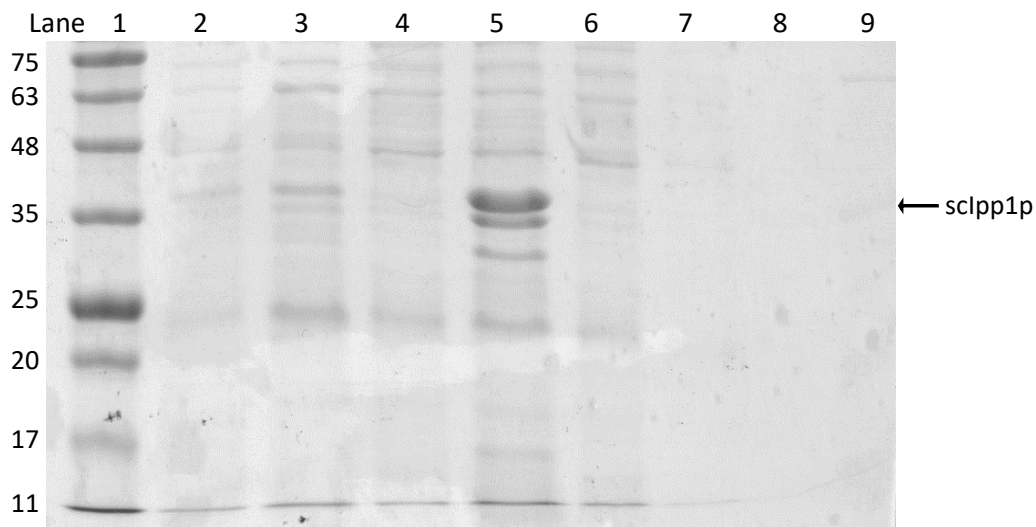


**Figure 5. Acrylamide (10% w/v) gel electrophoresis analysis of scIpp1p fractions induced with 0.2 µg/mL UV-exposed tetracycline from column purification.** scIpp1p was expressed in *E. coli* RIPL cells. The soluble fraction was passed through a 1 mL Strep-Tactin XT Superflow column and eluted with BXT buffer. Protein was stained using Coomassie Brilliant Blue R-250. Lane 1: MBI Rainbow Prestained Protein Evolution Ladder (5 µL); lane 2: pre-induction cell pellet (10 µg); lane 3: post-induction cell pellet (10 µg); lane 4: soluble fraction (10 µg); lane 5: insoluble fraction (10 µg); lane 6: non-binding eluate (10 µg); lane 7: wash (10 µg), lane 8: elution fraction (2 µg); lane 9: elution fraction (10 µg).

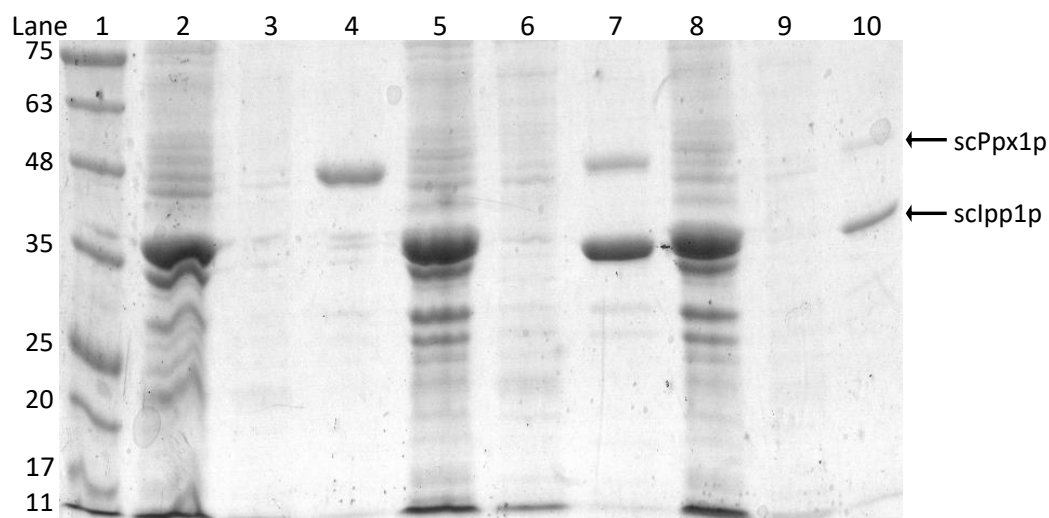


**Figure 6. Acrylamide (10% w/v) gel electrophoresis analysis of scPpx1p fractions induced with 0.2  $\mu\text{g}/\text{mL}$  anhydrotetracycline from column purification.** scPpx1p was expressed in *E. coli* RIPL cells. The soluble fraction was passed through a 1 mL Strep-Tactin XT Superflow column and eluted with BXT buffer. Separate protein expression trials are denoted through numbering. Protein was stained using Coomassie Brilliant Blue R-250. Lane 1: MBI Rainbow Prestained Protein Evolution Ladder (5  $\mu\text{L}$ ); lane 2: insoluble fraction 1 (10  $\mu\text{g}$ ); lane 3: non-binding eluate 1 (10  $\mu\text{g}$ ); lane 4: elution fraction 1 (5  $\mu\text{g}$ ); lane 5: insoluble fraction 2 (10  $\mu\text{g}$ ); lane 6: non-binding eluate 2 (10  $\mu\text{g}$ ); lane 7: elution fraction 2 (5  $\mu\text{g}$ ), lane 8: insoluble fraction 3 (10  $\mu\text{g}$ ); lane 9: non-binding eluate 3 (10  $\mu\text{g}$ ); lane 10: elution fraction 3 (5  $\mu\text{g}$ ).

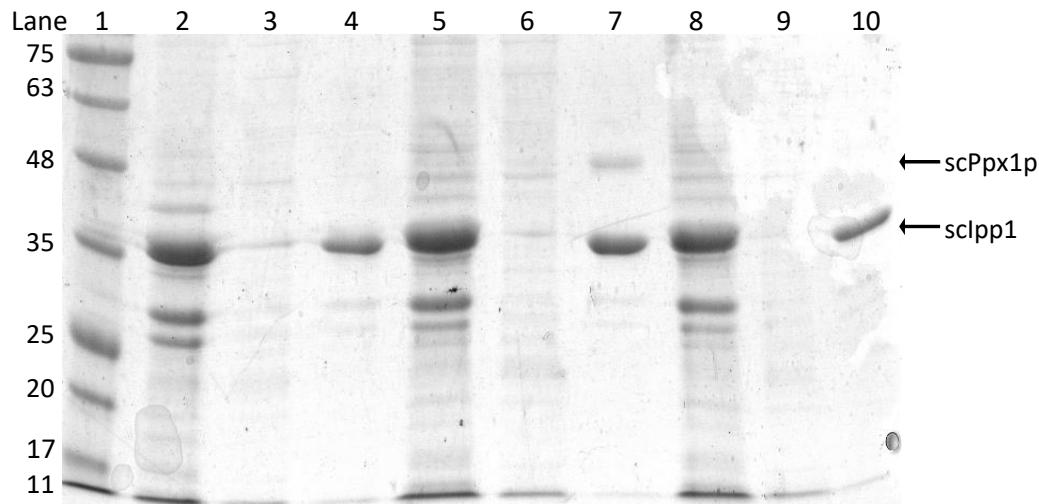


**Figure 7. Acrylamide (10% w/v) gel electrophoresis analysis of sclpp1p fractions induced with 0.2  $\mu\text{g}/\text{mL}$  anhydrotetracycline from column purification.** sclpp1p was expressed in *E. coli* RIPL cells. The soluble fraction was passed through a 1 mL Strep-Tactin XT Superflow column and eluted with BXT buffer. Separate protein expression trials are denoted through numbering. Protein was stained using Coomassie Brilliant Blue R-250. Lane 1: MBI Rainbow Prestained Protein Evolution Ladder (5  $\mu\text{L}$ ); lane 2: insoluble fraction 1 (10  $\mu\text{g}$ ); lane 3: non-binding eluate 1 (10  $\mu\text{g}$ ); lane 4: elution fraction 1 (5  $\mu\text{g}$ ); lane 5: insoluble fraction 2 (10  $\mu\text{g}$ ); lane 6: non-binding eluate 2 (10  $\mu\text{g}$ ); lane 7: elution fraction 2 (5  $\mu\text{g}$ ), lane 8: insoluble fraction 3 (10  $\mu\text{g}$ ); lane 9: non-binding eluate 3 (10  $\mu\text{g}$ ); lane 10: elution fraction 3 (5  $\mu\text{g}$ ).

### Specific enzyme activity assays

After the identities of the expressed proteins were confirmed through SDS-PAGE analysis, the specific activities of each scPpx1p and scIpp1p expression were determined, where one unit (U) of enzyme activity is equivalent to 1  $\mu\text{mol}$  of  $\text{P}_i$  released per min at 37°C for scIpp1p and equivalent to 1 pmol of  $\text{P}_i$  released per min for scppx1p (41). Calculated scPpx1p activities were  $1.860 \times 10^7$  U/mg for the TC-induced eluates and  $4.475 \times 10^7$  U/mg,  $4.374 \times 10^7$  U/mg, and  $5.801 \times 10^6$  U/mg for the tested AHTC-induced eluates. Calculated scIpp1p activities were 92.18 U/mg for the TC-induced eluates and 498.8 U/mg, 603.5 U/mg, and 423.0 U/mg for each tested AHTC-induced eluate (in the same order as protein expression trials using AHTC). Using these calculated activities normalized to total protein content in each elution fraction, the total amount of scPpx1p that was expressed and purified from all protein expression trials was found to be  $5.52 \times 10^8$  U and the total amount of scIpp1p that was expressed and purified was found to be  $4.15 \times 10^6$  U.

### Analysis of known polyphosphate amounts

To assess the accuracy of Christ and Blank's enzymatic molybdenum blue assay and the purified enzymes' ability to digest polyP into  $\text{P}_i$ , polyP-12 standards of known amounts (50-200  $\mu\text{M}$ ) were prepared and used as samples to confirm that their concentrations could be measured. This was done separately with each enzyme expression. The UV-exposed TC-induced enzymes were able to accurately measure the concentrations of the polyP-12 spikes with differences in the measured  $\text{P}_i$  concentrations depending on whether scPpx1p and scIpp1p or only scPpx1p enzymes were used (Table 1). The differences in these measurements allowed for the calculation of the length of the polyP chains in polyP-12 according to equation provided by Christ and Blank (41):

$$\text{average polyP chain length} = \frac{2 \times (\text{scPpx1p digestible polyP} - \text{blank } \text{P}_i [\mu\text{M } \text{P}_i])}{(\text{total polyP-scPpx1p digestible polyP } [\mu\text{M } \text{P}_i])} + 2$$

This equation allowed the average length of the polyP-12 used to be calculated, giving an average length of  $11.85 \pm 1.85$   $\text{P}_i$  units.

The AHTC-induced enzymes were also able to accurately measure the concentrations of the polyP-12 spikes, but there was no difference between the scPpx1p only and both scPpx1p and scIpp1p containing wells (Table 2). This indicates that the purified scPpx1p is contaminated with scIpp1p.

**Table 1. The measured and calculated phosphate concentrations ( $P_i$ ) ( $\mu\text{M}$ ) of sodium hexametaphosphate (polyP-12) standards of known concentrations digested with UV-exposed tetracycline induced enzymes. PolyP-12 standards were made in MQ water and treated like samples. Measured A882 was converted to  $P_i$  using a  $\text{Na}_2\text{PO}_4$  standard curve ( $y=0.0054x+0.0316$  where  $y$  is A882 and  $x$  is  $[P_i]$ ,  $R^2=0.9841$ ). A882 was measured using a Molecular Devices M3 spectrophotometer and the Softmax Pro program and data analysis was done with Excel.**

Sample	Blank	scPpx1p					scPpx1p and sclpp1p				
		200 $\mu\text{M}$	180 $\mu\text{M}$	160 $\mu\text{M}$	100 $\mu\text{M}$	50 $\mu\text{M}$	200 $\mu\text{M}$	180 $\mu\text{M}$	160 $\mu\text{M}$	100 $\mu\text{M}$	50 $\mu\text{M}$
A882	0.1003	0.9532	0.8066	0.7579	0.5156	0.2996	1.1084	0.9939	0.8834	0.5728	0.3508
	0.0984	0.9325	0.8562	0.7722	0.5187	0.2924	1.0916	1.0199	0.8845	0.5818	0.3507
	0.0952	0.952	0.8203	0.733	0.5088	0.2923	1.1101	1.0208	0.8656	0.5899	0.34
Measured blank	12.72	170.7	143.5	134.5	89.63	49.63	199.4	178.2	157.7	100.2	59.11
corrected $[P_i]$	12.37	166.8	152.7	137.1	90.2	48.3	196.3	183	157.9	101.9	59.09
( $\mu\text{M}$ )	11.78	170.4	146.1	129.9	88.37	48.28	199.7	183.2	154.4	103.4	57.11
Average $[P_i]$	12	169	147	134	89	49	198	181	157	102	58
( $\mu\text{M}$ )											

**Table 2. The measured and calculated phosphate concentrations (Pi) (μM) of sodium hexametaphosphate (polyP-12) standards of known concentrations digested with anhydrotetracycline (AHTC) induced enzymes. PolyP-12 standards were made in MQ water and treated like samples. Measured A882 was converted to Pi using a Na<sub>2</sub>PO<sub>4</sub> standard curve ( $y=0.0058x+0.0112$  where y is A882 and x is [Pi],  $R^2=0.9832$ ). A882 was measured using a Molecular Devices M3 spectrophotometer and the Softmax Pro program and data analysis was done with Excel. The scPpx1p only samples from the AHTC induction were included to demonstrate the scPpx1p the contamination of eluates with sclpp1p.**

Sample	Blank	AHTC #1						AHTC #2						AHTC #3									
		scPpx1p			scPpx1p and sclpp1p			scPpx1p and sclpp1p			scPpx1p and sclpp1p			scPpx1p and sclpp1p			scPpx1p and sclpp1p						
		200 μM	180 μM	160 μM	200 μM	180 μM	160 μM	200 μM	180 μM	160 μM	200 μM	180 μM	160 μM	200 μM	180 μM	160 μM	200 μM	180 μM	160 μM	100 μM			
A882	0.0695	1.206	1.093	0.979	1.225	1.106	1.014	1.24	1.124	0.989	1.247	1.137	0.969	1.24	1.106	0.994	1.24	1.124	0.989	1.252	1.1	0.996	0.653
Measured [Pi] (μM)	8.82	205.1	185.7	166	208.4	187.9	172.1	210.9	191	167.7	212.1	193.2	164.3	210.9	188	168.7	212.6	192.7	169.3	212.9	186.8	169	110.1
Average [Pi] (μM)	9	207	186	167	210	187	171	211	191	167	210.9	188	168.7	211	189	170	211	189	170	211	189	170	111
Blank corrected [Pi] (μM)	-	198	177	158	201	178	162	202	182	158	202	182	158	202	180	161	202	180	161	202	180	161	101

### Testing of ascorbate assay robustness and ruggedness

The interference effects of extraction and digestion materials on the colorimetric response of the ascorbate assay were measured by preparing a  $\text{NaH}_2\text{PO}_4$  (Sigma #S9763) standard curve in extraction buffer instead of MQ water. The resulting curve had a very similar y-intercept to the MQ water standard curve, but a slightly more gradual slope of  $A_{882}$  response to  $\text{P}_i$  concentration (Figure 8). This indicates that the response of the ascorbate assay to  $\text{P}_i$  concentration is not greatly affected by buffer contamination, even at maximum buffer contamination, but extracted samples will be diluted in MQ water to ensure there are no interfering effects regardless.

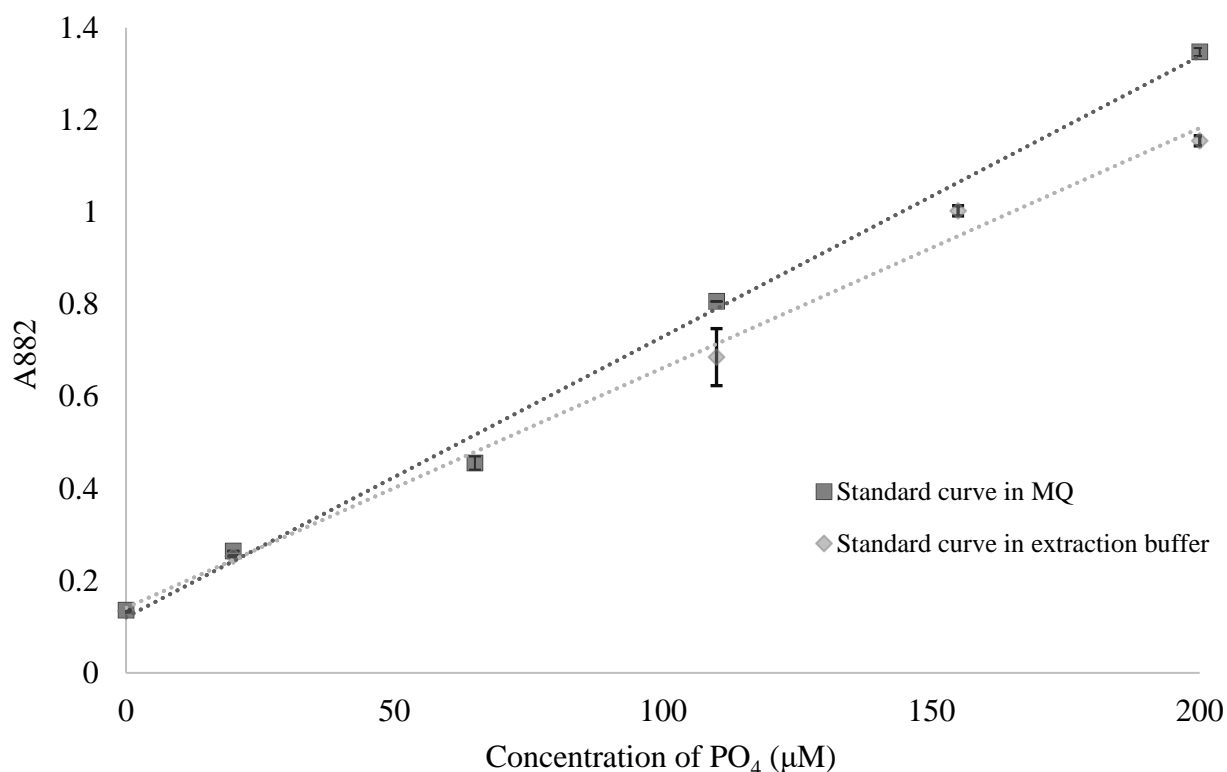


**Figure 8. Standard curve of the ascorbate assay reaction with  $\text{Na}_2\text{PO}_4$  standards made with MQ water (square) and extraction buffer (diamond) at an absorbance of 882 nm ( $A_{882}$ ).** The linear regression of the MQ water standard curve was  $y=0.0061x+0.1208$  and the coefficient of correlation was 0.9950. The linear regression of the extraction buffer standard curve was  $y=0.0052x+0.1413$  and the coefficient of correlation was 0.9942.

The response of the molybdenum blue assay was also tested in varying dilutions of extraction and digestion material and varying concentrations of  $\text{P}_i$  to ensure that there was no discernible change in response that would result from diluting samples at different amounts to

reach a measurable  $P_i$  concentration. The results indicated that as a sample of spiked extraction buffer is diluted, the measured  $A_{882}$  and calculated concentration of  $P_i$  is lowered at a rate proportional to the amount of dilution (Figure 9). Different diluted extraction buffer samples were also spiked with a constant amount of  $P_i$  to ensure that response remained stable as the concentration of buffer contaminants varied, which the test confirmed (Figure 9).

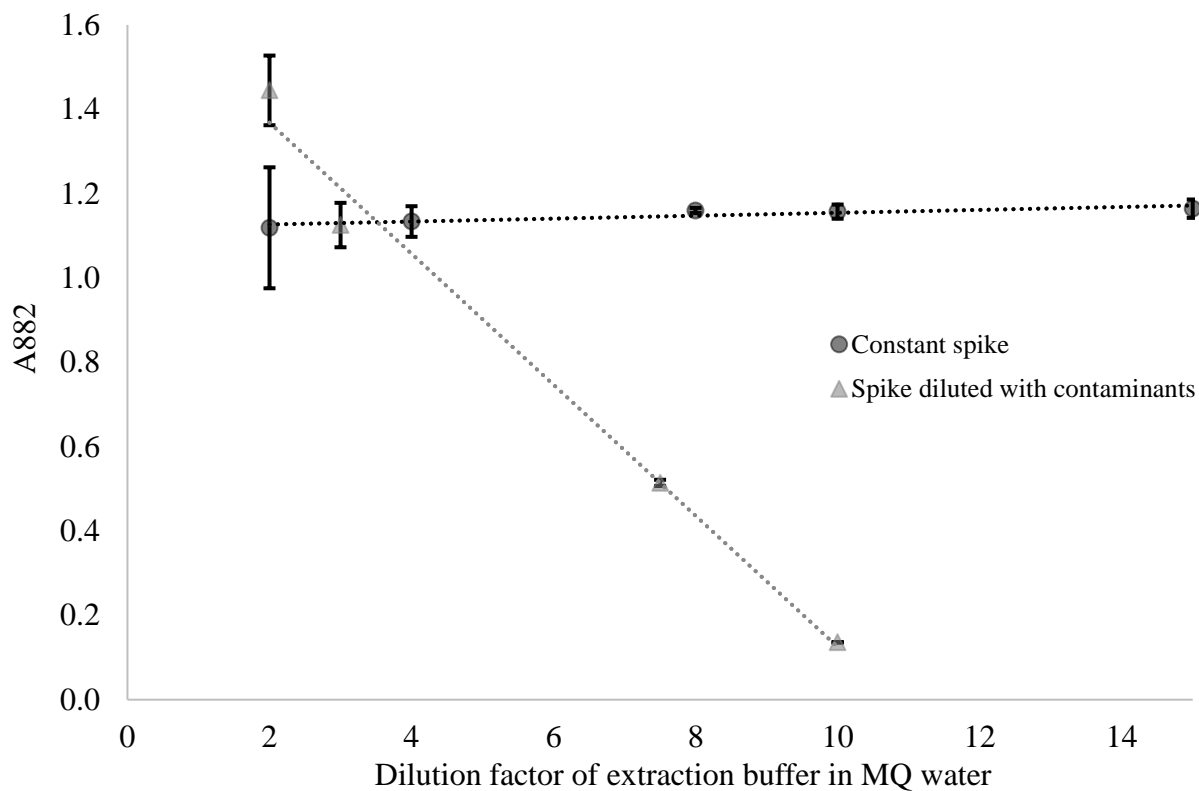


**Figure 9. Ascorbate assay response to varying phosphate ( $P_i$ ) concentrations with varying buffer contamination levels (triangle) and to constant  $P_i$  concentrations with varying buffer contamination (circle) at an absorbance of 882 nm ( $A_{882}$ ).** Extraction buffer spikes ( $400 \mu\text{M}$  with  $P_i$ ) and blanks were run through the digestion and incubation process before dilution (1:2 to 1:15) with MQ water, at which point the blank dilutions were spiked with a constant amount of  $P_i$  ( $180 \mu\text{M}$ ). The linear regression of the diluted spike samples was  $y=-0.1554x+1.6792$  and the coefficient of correlation was 0.9870. The linear regression of the constant spike samples was  $y=0.0035x+1.12$  and the coefficient of correlation was 0.8174.

The effects of buffer contamination on enzyme activity were measured by spiking extraction buffer dilutions with constant amounts of polyP-12 and comparing the resulting  $A_{882}$  values and calculated  $P_i$  concentrations. It was determined that all samples extracted following Christ and Blank's optimized polyP extraction protocol should be diluted at least 1:4 with MQ

water prior to the addition of enzymes and incubation due to the 1:2 dilution leading to an incomplete digestion (Figure 10).

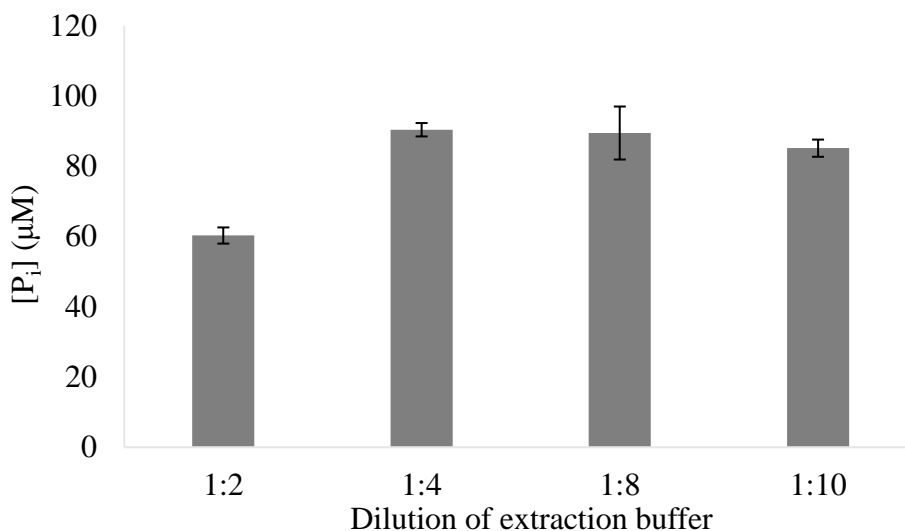


**Figure 10. Enzymatic capacity of scIpp1p and scPpx1p to digest sodium hexametaphosphate (polyP-12) spikes at differing levels of buffer contamination.** All dilutions were spiked with polyP-12 prior to digestion and incubation (90 µM as phosphate (P<sub>i</sub>)). Extraction buffer was diluted with MQ water.

### **Optimized Christ and Blank polyphosphate extraction protocol trials**

Of the multiple extractions conducted with polyP-12 or *Polysiphonia*, only once was polyP able to be quantified. In total, one polyP-12 sample was measurably extracted. Changes were made to the outlined protocol to attempt to increase the rate of measurable extraction, including changing the point at which the polyP sample is added, adding a buffer to raise the pH of the phenol used, and including or omitting the phase lock gel to see if it was interfering with polyP partitioning. None of the changes to the methods resulted in detection of polyP from standards or samples, so a different method was chosen for final analysis of biological samples.

### **Bru *et al.* polyphosphate extraction protocol trial**

The Bru *et al.* method was used to process three samples of *Synechocystis* sp. PCC6803, three known polyP-45 samples, and two blank samples. PolyP was unable to be measurably extracted from polyP-45 samples but was measurable in all three *Synechocystis* sp. PCC6803 samples. In the wells with no enzyme treatment, the measured background P<sub>i</sub> concentrations were 72.28, 115.41, and 86.77 µM, and in the wells treated with scPpx1p and scIpp1p, the measured total P<sub>i</sub> concentrations were 159.35, 222.23, and 165.70 µM. The concentration of P<sub>i</sub>

from the hydrolysis of polyP was calculated to be 87.06, 106.81, and 78.93  $\mu\text{M}$ . Aliquots from each sample tested were saved for later chlorophyll content analysis.

## Discussion

### Expression and purification of scPpx1p and scIpp1p

The *E. coli* RIPL cells were successfully transformed with pDNA and proteins were able to be expressed and purified from them. The observed protein size of scIpp1p was between 33.1 kDa (Figure 5) and 36.7 kDa (Figure 7), only 3.8% and 13.7% different than the expected size of 32 kDa (45). The observed size of scPpx1p was more consistent, being between 48.3 kDa (Figure 4) and 48.7 kDa (Figure 6), a 7.1% and 7.9% difference from the expected size of 45 kDa (35). The identification of the expressed and purified enzymes as scPpx1p and scIpp1p was confirmed using specific enzyme activity assays that could measure the polyphosphatase and pyrophosphatase activity of each enzyme through the measured release of  $\text{P}_i$  from polyP or  $\text{PP}_i$  within a set time frame. The measured specific enzyme activity for AHTC induced scPpx1p, excluding the much less active third AHTC induction, was an average of  $4.42 \times 10^7 \pm 5.05 \times 10^5$  U/mg and the value reported by Christ and Blank was  $7.5 \times 10^8$  U/mg. The specific enzyme activity for the AHTC induced scIpp1p produced was an average  $508 \pm 74$  U/mg and the reported activity was 895 U/mg (41). In both cases, the scPpx1p was the more active of the enzymes, but the enzymes produced for this study have less activity than the reported value by over a magnitude. The scIpp1p produced also shows less activity than the reported value. The most likely explanation for this disparity is the presence of contaminating proteins in the purified protein eluates (Figure 6, 7), which would increase the measured mass of total protein in each eluate but would not increase the activity of those eluates, reducing the calculated specific activity of each enzyme.

The contamination of the second and third ACTH-induced protein expressions was first seen in the SDS-PAGE analysis of the eluates from protein purification (Figure 6, 7) and later confirmed by testing these eluates for the activity of the contaminating enzyme and measuring pyrophosphatase activity in the scPpx1p eluates and polyphosphatase activity in the scIpp1p eluates. The main contaminating protein band being one that belongs to another enzyme with a Twin-Strep-tag makes sense, given that all proteins that occur naturally in *E. coli* lack this tag and should have been washed out of the column with buffer W before elution with buffer BXT.

Since all proteins were expressed from the same *E. coli* RIPL cells transformed with the additional pDNA produced (and not the original plasmids sent by Jonas Christ), the contamination does not stem from an error when producing the pDNA. The TC-induced proteins and first of the AHTC-induced proteins being uncontaminated confirm this. The last two AHTC-induced protein expressions were performed on the same day to increase the amount of enzyme produced (after several failed protein expressions due to slow *E. coli* growth), making it more likely that a single error when pipetting or when harvesting the cells would be able to contaminate multiple cultures.

The contamination of the purified enzyme eluates had no negative effect on their intended enzyme activities and so they were still able to be used for their intended purposes. The only downside to the contamination was that average polyP chain length was unable to be calculated, due to the equation relying on the difference between the measured  $P_i$  concentrations upon treatment with only scPpx1p and both scPpx1p and scIpp1p. This downside did not have a great effect on the overall project since only one biological sample was able to be analyzed, preventing the comparison of polyP chain length between species.

### **Analysis of known polyphosphate amounts**

The ability of the ascorbate acid assay to measure polyP concentrations once broken down into  $P_i$  was surprisingly accurate. The highest difference between the target  $P_i$  and measured  $P_i$  concentration was 14.8%, between the spike of 50  $\mu\text{M}$  and measured concentration of 58  $\mu\text{M}$  (Table 1). Christ and Blank reported that the assay was most accurate the closer to 200  $\mu\text{M}$  the  $P_i$  concentration was, so this difference could be due to 50  $\mu\text{M}$  being the farthest concentration tested from 200  $\mu\text{M}$  (41). The rest of the measured values from the UV-exposed TC induced enzymes had a less than 2% difference from the known polyP concentration. The AHTC induced enzymes followed a similar trend, with each measured concentration having a less than 1.5% difference from the known concentration (Table 2). This accuracy demonstrates the ability of the ascorbate acid assay to identify the amount of  $P_i$  that once belonged to polyP in a sample and confirms that it is a good method for enzymatically breaking down and measuring polyP.

## Effects of extraction materials on assay response

The ability of the ascorbate acid assay outlined by Christ and Blank was tested at various levels of contamination by the extraction and digestion buffer materials as well as different concentrations of  $P_i$  and polyP (41). This was done because the original assay was only ever tested on *S. cerevisiae*, a species that, when being grown for use in such assays, typically has a much higher biomass than any aquatic or marine species would. This means that large dilutions in MQ water would have to be done to bring polyP concentrations down to an amount measurable by the assay, with the target always being around 180  $\mu\text{M}$ . These dilutions would prevent any interference with the assay on the part of contaminants due to how little contaminant would remain compared to the MQ water in the diluted sample, and so all samples would behave similarly or identically to the standard curve (a  $P_i$  salt dissolved in MQ water). Since phytoplankton are difficult to grow to similar densities and nearly impossible to collect from the wild in such high densities, phytoplankton samples would not have to be diluted to the same amount to fall within a measurable range of polyP, leaving the potential for contaminants and matrix effects to interfere with the assay. The extraction buffer, based on its smell and the extraction process, contains trace amounts of phenol and likely chloroform as well, two compounds with far different densities and polarities than water which could interfere with the response of the assay if left undiluted.

The slope of the standard curve in blank extraction buffer is less steep than that of the standard curve in MQ water (Figure 8), showing that this contamination does have some effect on the analyte response of the assay and reduces its absorbance slightly. However, the y-intercepts of both standard curves are very similar and any dilution with MQ water that the sample undergoes would make the response more similar to that of the standard curve, meaning contamination effects will be able to be mitigated with sample dilution.

The conclusion that samples would be able to be safely diluted were reached by looking at the assay response at different contamination levels by diluting the extraction buffer in MQ water (Figure 9). At lower dilutions, the results were more variable for the same  $P_i$  concentration but as contaminant concentration went down, the analyte response became less variable and slightly more intense. As both  $P_i$  and contaminant concentration were diluted, the analyte signal was reduced at a predictable and reasonable rate and the resulting regression was linear. This indicates that the difference in analyte response between the standard curve and the samples can

be reduced through sample dilution and that diluting samples with MQ water will not have any effect on the signal that would reduce the reliability of the assay.

### **Effects of extraction materials on enzyme activity**

The trace amounts of phenol and chloroform had a negative effect on the capacity of scIpp1p and scPpx1p to digest polyP-12 samples (Figure 10). At any dilution of the extraction buffer less than 1:4 in MQ water, the activities of the enzymes were inhibited by these contaminants and were unable to fully digest the polyP-12 present in the sample within the hour in which the 96-well microplate is incubated at 37°C. Reduced enzyme activity is likely due to any inhibition from the corrosive and protein degenerating effects that any contaminating phenol would present to the purified enzymes (46). It was concluded that all samples that had gone through Christ and Blank's optimized extraction protocol would be diluted at least 1:4 in MQ water to avoid this interference.

### **Polyphosphate in *Polysiphonia lanosa***

The Christ and Blank extraction method was unsuccessful in extracting polyP from the *Polysiphonia* samples tested. Since the protocol in their published paper was followed exactly (with the addition of bead beating after the addition of ME-buffer to guarantee the breaking of the cell wall), it seemed unlikely that the extraction of polyP from a biological sample would have failed. Since the nutrient availability at the time of collection is unknown and the *Polysiphonia* was growing on top of another algae, it is probable that it was competing for nutrients and there was not enough P available to form significant amounts of polyP. A lack of polyP to be extracted would explain why the extraction process failed with biological samples. If this extraction were to be attempted with lab-grown cultures with an abundance of nutrients available to them polyP production could be guaranteed and the Christ and Blank extraction method could be attempted again on a biological sample.

### **Troubleshooting the Christ and Blank extraction method**

The optimized extraction protocol published by Christ and Blank was ineffective when attempted with polyP-12 and in the end polyP was only successfully partitioned to the top aqueous phase once for later quantitation (40). It was immediately evident that the polyP was not partitioning to the top aqueous phase during extraction because of the lack of measurable  $P_i$  in the samples. If there was some form of contaminant in the top phase causing the polyP to fully

hydrolyze into  $P_i$  units, these should have been measurable in the ascorbate assay from the reaction between solution B and  $P_i$ . If any polyP had been present in the aqueous phase, the diluted extraction samples tested should have given a measurable signal due to the dilution allowing the enzymes to digest the polyP uninhibited by any extraction buffer contaminants. The reason for the failure of this extraction was unknown, so multiple changes were made between extractions to identify the reason for failure.

The phenol that was originally used (BioShop #PHE510) was not buffered with the additional TRIS buffer provided by BioShop Canada, meaning its pH may have only been 6.6 and not the pH needed for the extraction (pH 7.5-8.0). Linear polyP exhibits a weakly acidic H at either end of its chain with a lower pKa range around 7, so at a pH below this the polyP could be protonated, rendering it more non-polar and thus more able to partition to the lower organic phase (47). However, once the additional TRIS buffer was added to the phenol and mixed (theoretically bringing the pH to an advertised 7.9), the polyP of the following extractions was still not partitioning to the aqueous phase.

It was also thought that the polyP standards lost during extraction may be caught at the interphase where the phase lock gel was located. To test this, extractions with and without the phase lock gel were run concurrently. One of the extractions with the phase lock gel was the only one to show a successful polyP-12 extraction, so it was concluded that the presence of phase lock gel was not interfering with polyP partitioning. The phase lock gel was occasionally found at both the interphase and the bottom of the reaction tube after centrifuging. This should not have occurred since the density of the phase lock gel should be between that of water and the phenol and chloroform mixture. New phase lock gel was made and the amount of gel forming a pellet was reduced, but a pellet still formed.

It was concluded that the polyP from the standards was partitioning to the lower organic layer for unknown reasons. Since the optimized Christ and Blank extraction protocol was not going to be a viable option for the analysis of biological samples through spike and recovery assays, the Bru *et al.* extraction protocol that the optimized protocol was based on was tested to determine if it could successfully extract polyP from standards and biological samples (38).

### **Polyphosphate in *Synechocystis* sp. PCC6803**

The Bru *et al.* extraction method was able to successfully extract polyP from *Synechocystis* sp. PCC6803, confirming its presence in the species and that the Bru *et al.* method

can extract polyP from biological samples. An estimate of total P content in the samples was made to ensure only an amount that would fall within the standard curve would be extracted, but background  $P_i$  was higher than anticipated.

The high concentration of background  $P_i$  measured in *Synechocystis* samples was not present in *Polysiphonia* samples. The reason for this disparity may be that the culture samples were grown in high  $P_i$  media, concentrated by centrifugation which could have caused  $P_i$  leakage from stressed or lysed cells, and that some media remained in the collected pellets. Precipitated polyP was also dried in the presence of supernatant to avoid losing the pellet, meaning it could contain  $P_i$  free in the cells, from the media used, or from the hydrolysis of RNA, DNA, or ATP (48). The drying overnight could also have resulted in polyP breakdown, contributing to the background  $P_i$  and reducing the measurable polyP. Background  $P_i$  from these sources would be present in both enzyme-treated and blank samples and detectable by the colorimetric molybdenum blue assay (47). Regardless of the source of the background  $P_i$ , exopolyphosphatase from *S. cerevisiae* only targets polyP as a substrate, so any additional  $P_i$  detected in enzyme-treated samples are assumed to be from polyP.

### **Extraction of polyphosphate standards**

Both extraction methods tested successfully extract polyP from biological samples, but are unable to extract polyP standards, either polyP-12 or polyP-45. The inability of these methods to extract polyP standards was not mentioned in either papers outlining the Christ and Blank extraction or the Bru *et al.* extraction, and it is unknown whether these methods were tested on standards as well as biological samples or not. Natural polyP can be thousands of  $P_i$  units long, whereas the tested standards only had chain lengths of 12 and 45. Biological polyP occurring in yeast vacuoles has been shown to be associated with several cations, including  $Mg^{2+}$ ,  $Mn^{2+}$ ,  $K^+$ , and  $Fe^{2+}$  cations, arginine, and other cationic amino acids (49, 50). PolyP *in vivo* can also be associated with proteins and is often found in membrane-bound granules (25, 51, 52). The polyP standards used only contained  $Na^+$  as a cation and no added proteins or lipids. These multiple factors mark clear differences between biological polyP and the standards used that could have affected extraction.

The differences between these two forms of the polymer that prevent polyP standards from being extracted while permitting biological polyP to be extracted are currently unknown. This inability to extract polyP standards prevents the use of spike and recovery assays to

determine extraction efficiency and absolute accuracy of these assays and brings into question the ability of these methods to extract naturally occurring polyP with a shorter chain length like that of the polyP standards.

### **Future Directions**

In this study, it was determined that while the molybdenum blue assay outlined by Christ and Blank is an accurate assay, both in quantifying polyP and measuring the length of polyP chains, the optimized polyP extraction protocol by Christ and Blank and that by Bru *et al.* do not reliably extract polyP standards. While these methods may be the gold standard for polyP extraction from biological samples, this inability to extract polyP standards prevents extraction efficiency and accuracy from being measured through spike and recovery tests using polyP standards. In order to enable and advance future studies on polyP, a polymer found in all living organisms (21), a unified protocol that is successful when used to extract and quantify polyP from a multitude of sources, biological or not, will have to be developed.

PolyP was successfully extracted from *Synechocystis* sp. PCC6803. The modeling of polyP content and P storage in this species would be useful, given its identity as one of the most highly studied types of cyanobacteria and a model microorganism for the study of photosynthesis, C sequestration, and N assimilation (53). If the effects of P availability and polyP storage on these other processes can be identified in *Synechocystis* sp. PCC6803, it could provide insight into the greater role P storage and availability plays in global ocean productivity and biogeochemical cycling.

Future directions for this project include the characterization of P use within *Synechocystis* sp. PCC6803 and phytoplankton by comparing measured polyP content to other major pools of cellular P like RNA, DNA, and phospholipids. Coupled with measurements of total cellular P, this could serve to model P use in phytoplankton and, if the sum of P content in major cellular pools and polyP accounts for the majority of total P, act as an independent method to confirm the accuracy of polyP extraction and measurement. The polyP extracted from *Synechocystis* could also be characterized with SDS-PAGE analysis or <sup>31</sup>P-NMR to assess polyP chain length and compare this to the standards used, or Raman microspectroscopy could be used to measure polyP and other major macromolecules within individual cells (39). The organic phase from failed extractions should also be examined to locate the lost polyP standards and

determine why biological polyP can be extracted but the standards cannot, especially since every other aspect of the quantification methods worked in an identical manner with both types of polyP. If standards were unable to be extracted, these extraction methods may also be unable to extract natural polyP chains with a similar length to the standards. Examining the differences between natural polyP and polyP standards could be the key to identifying why extraction failed and developing methods that would work for biological samples and standards alike.

The development of reliable polyP extraction and quantification methods would facilitate research on the contributions of polyP to overall phytoplankton metabolism of P, an element that often limits growth across the ocean and over geological time. Accurately quantifying polyP will also help to elucidate the functions of this poorly understood polymer, which appears to be a ubiquitous and essential component of all known life.

## Literature Cited

1. C. S. Reynolds, P. S. Davies, Sources and bioavailability of phosphorus fractions in freshwaters: a British perspective. *Biol Rev.* **76**, 27–64 (2001).
2. K. C. Ruttenberg, in *Treatise on Geochemistry*, H. D. Holland, K. K. Turekian, Eds. (Pergamon, Oxford, 2003; <https://www.sciencedirect.com/science/article/pii/B0080437516081536>), vol. 8, pp. 585–643.
3. D. Sayantan, S. S. Das, in *Contemporary Topics about Phosphorus in Biology and Materials* (2020; <https://www.intechopen.com/chapters/71223>).
4. M. L. Delaney, Phosphorus accumulation in marine sediments and the oceanic phosphorus cycle. *Global Biogeochem Cycles.* **12**, 563–572 (1998).
5. D. Cordell, J.-O. Drangert, S. White, The story of phosphorus: Global food security and food for thought. *Glob Environ Change.* **19**, 292–305 (2009).
6. J. Grantham, Be persuasive. Be brave. Be arrested (if necessary). *Nature.* **491**, 303–303 (2012).
7. T. Worstall, A shortage of fertilizer resources? *Nature.* **493**, 163–163 (2013).
8. S. P. Slocombe, T. Zúñiga-Burgos, L. Chu, N. J. Wood, M. A. Camargo-Valero, A. Baker, Fixing the broken phosphorus cycle: Wastewater remediation by microalgal polyphosphates. *Front Plant Sci.* **11**, 982 (2020).
9. C. P. Vance, C. Uhde-Stone, D. L. Allan, Phosphorus acquisition and use: critical adaptations by plants for securing a nonrenewable resource. *New Phytol.* **157**, 423–447 (2003).
10. A. H. W. Beusen, A. F. Bouwman, L. P. H. Van Beek, J. M. Mogollón, J. J. Middelburg, Global riverine N and P transport to ocean increased during the 20th century despite increased retention along the aquatic continuum. *Biogeosciences.* **13**, 2441–2451 (2016).
11. A. Paytan, K. McLaughlin, The oceanic phosphorus cycle. *Chem Rev.* **107**, 563–576 (2007).

12. Canadian Council of Ministers of the Environment, Canadian Water Quality Guidelines for the Protection of Aquatic Life - Phosphorus: Canadian Guidance Framework for the Management of Freshwater Systems. *Canadian Environmental Quality Guidelines*, 6 (2004).
13. M. G. M. G. Penido, U. S. Alon, Phosphate homeostasis and its role in bone health. *Pediatr Nephrol.* **27**, 2039–2048 (2012).
14. N. N. Rao, M. R. Gómez-García, A. Kornberg, Inorganic polyphosphate: Essential for growth and survival. *Annu Rev Biochem.* **78**, 605–647 (2009).
15. R. L. Bielecki, I. B. Ferguson, in *Inorganic Plant Nutrition*, A. Läuchli, R. L. Bielecki, Eds. (Springer, Berlin, Heidelberg, 1983; [https://doi.org/10.1007/978-3-642-68885-0\\_15](https://doi.org/10.1007/978-3-642-68885-0_15)), *Encyclopedia of Plant Physiology*, pp. 422–449.
16. F. Ardito, M. Giuliani, D. Perrone, G. Troiano, L. L. Muzio, The crucial role of protein phosphorylation in cell signaling and its use as targeted therapy (Review). *Int J Mol Med.* **40**, 271–280 (2017).
17. H. Gu, S. Lalonde, S. Okumoto, L. L. Looger, A. M. Scharff-Poulsen, A. R. Grossman, J. Kossmann, I. Jakobsen, W. B. Frommer, A novel analytical method for *in vivo* phosphate tracking. *FEBS Letters.* **580**, 5885–5893 (2006).
18. C. Tarayre, H.-T. Nguyen, A. Brognaux, A. Delepierre, L. De Clercq, R. Charlier, E. Michels, E. Meers, F. Delvigne, Characterisation of phosphate accumulating organisms and techniques for polyphosphate detection: A review. *Sensors.* **16**, 797 (2016).
19. T. M. Livermore, J. R. Chubb, A. Saiardi, Developmental accumulation of inorganic polyphosphate affects germination and energetic metabolism in *Dictyostelium discoideum*. *Proc Natl Acad Sci U S A.* **113**, 996–1001 (2016).
20. A. Kornberg, Inorganic polyphosphate: toward making a forgotten polymer unforgettable. *J Bacteriol* (1995), doi:10.1128/jb.177.3.491-496.1995.
21. R. Gerasimaitė, A. Mayer, Enzymes of yeast polyphosphate metabolism: structure, enzymology and biological roles. *Biochem Soc Trans.* **44**, 234–239 (2016).
22. A. Kornberg, N. N. Rao, D. Ault-Riché, Inorganic polyphosphate: A molecule of many functions. *Annu Rev Biochem.* **68**, 89–125 (1999).

23. R. Manganelli, Polyphosphate and stress response in mycobacteria. *Mol Microbiol.* **65**, 258–260 (2007).
24. E. Sanz-Luque, D. Bhaya, A. R. Grossman, Polyphosphate: A multifunctional metabolite in cyanobacteria and algae. *Front Plant Sci.* **11**, 938 (2020).
25. M. J. Gray, W.-Y. Wholey, N. O. Wagner, C. M. Cremers, A. Mueller-Schickert, N. T. Hock, A. G. Krieger, E. M. Smith, R. A. Bender, J. C. A. Bardwell, U. Jakob, Polyphosphate is a primordial chaperone. *Mol Cell.* **53**, 689–699 (2014).
26. M. J. Gray, U. Jakob, Oxidative stress protection by polyphosphate-new roles for an old player. *Curr Opin Microbiol.* **24**, 1–6 (2015).
27. J. D. Liefer, A. Garg, M. H. Fyfe, A. J. Irwin, I. Benner, C. M. Brown, M. J. Follows, A. W. Omta, Z. V. Finkel, The macromolecular basis of phytoplankton C:N:P under nitrogen starvation. *Front Microbiol.* **10**, 763 (2019).
28. Y. Sekerci, S. Petrovskii, Mathematical modelling of plankton-oxygen dynamics under the climate change. *Bull Math Biol.* **77**, 2325–2353 (2015).
29. P. Martin, F. M. Lauro, A. Sarkar, N. Goodkin, S. Prakash, P. N. Vinayachandran, Particulate polyphosphate and alkaline phosphatase activity across a latitudinal transect in the tropical Indian Ocean. *Limnol Oceanogr.* **63**, 1395–1406 (2018).
30. L. Wang, J. Yan, M. J. Wise, Q. Liu, J. Asenso, Y. Huang, S. Dai, Z. Liu, Y. Du, D. Tang, Distribution patterns of polyphosphate metabolism pathway and its relationships with bacterial durability and virulence. *Front Microbiol.* **9** (2018) (available at <https://www.frontiersin.org/article/10.3389/fmicb.2018.00782>).
31. S. T. Dyhrman, in *The Physiology of Microalgae*, M. A. Borowitzka, J. Beardall, J. A. Raven, Eds. (Springer International Publishing, Cham, 2016; [https://doi.org/10.1007/978-3-319-24945-2\\_8](https://doi.org/10.1007/978-3-319-24945-2_8)), *Developments in Applied Phycology*, pp. 155–183.
32. T. Kulakovskaya, I. Kulaev, Enzymes of inorganic polyphosphate metabolism. *Prog Mol Subcell Biol.* **54**, 39–63 (2013).

33. M. P. Whitehead, P. Hooley, M. R. W Brown, Horizontal transfer of bacterial polyphosphate kinases to eukaryotes: implications for the ice age and land colonisation. *BMC Res Notes*. **6**, 221 (2013).
34. A. Bentley-DeSousa, M. Downey, Vtc5 is localized to the vacuole membrane by the conserved AP-3 complex to regulate polyphosphate synthesis in budding yeast. *mBio*. **12**, e00994-21.
35. T. V. Kulakovskaya, N. A. Andreeva, L. A. Ledova, L. P. Ryazanova, L. V. Trilisenko, M. A. Eldarov, Enzymes of polyphosphate metabolism in yeast: Properties, functions, practical significance. *Biochemistry (Mosc)*. **86**, S96–S108 (2021).
36. P. Martin, B. A. S. Van Mooy, Fluorometric quantification of polyphosphate in environmental plankton samples: Extraction protocols, matrix effects, and nucleic acid interference. *Appl Environ Microbiol*. **79**, 273–281 (2013).
37. A. Mullan, J. P. Quinn, J. W. McGrath, A nonradioactive method for the assay of polyphosphate kinase activity and its application in the study of polyphosphate metabolism in *Burkholderia cepacia*. *Anal Biochem*. **308**, 294–299 (2002).
38. S. Bru, J. Jiménez, D. Canadell, J. Ariño, J. Clotet, Improvement of biochemical methods of polyP quantification. *Microb Cell*. **4**, 6–15 (2016).
39. Š. Moudříková, A. Sadowsky, S. Metzger, L. Nedbal, T. Mettler-Altmann, P. Mojzeš, Quantification of polyphosphate in microalgae by Raman microscopy and by a reference enzymatic assay. *Anal Chem*. **89**, 12006–12013 (2017).
40. J. J. Christ, L. M. Blank, Analytical polyphosphate extraction from *Saccharomyces cerevisiae*. *Anal Biochem*. **563**, 71–78 (2018).
41. J. J. Christ, L. M. Blank, Enzymatic quantification and length determination of polyphosphate down to a chain length of two. *Anal Biochem*. **548**, 82–90 (2018).
42. T. Hasan, M. Allen, B. S. Cooperman, Anhydrotetracycline is a major product of tetracycline photolysis. *J Org Chem*. **50**, 1755–1757 (1985).
43. M. M. Bradford, A rapid and sensitive method for the quantitation of microgram quantities of protein utilizing the principle of protein-dye binding. *Anal Biochem*. **72**, 248–254 (1976).

44. T. Zor, Z. Selinger, Linearization of the Bradford protein assay increases its sensitivity: Theoretical and experimental studies. *Anal Biochem.* **236**, 302–308 (1996).
45. A. A. Baykov, A. S. Shestakov, Two pathways of pyrophosphate hydrolysis and synthesis by yeast inorganic pyrophosphatase. *Eur J Biochem.* **206**, 463–470 (1992).
46. M. Weber, M. Weber, V. Weber, in *Ullmann's Encyclopedia of Industrial Chemistry* (John Wiley & Sons, Ltd, 2020; [https://onlinelibrary.wiley.com/doi/abs/10.1002/14356007.a19\\_299.pub3](https://onlinelibrary.wiley.com/doi/abs/10.1002/14356007.a19_299.pub3)), pp. 1–20.
47. J. J. Christ, S. Willbold, L. M. Blank, Methods for the analysis of polyphosphate in the life sciences. *Anal Chem.* **92**, 4167–4176 (2020).
48. M. Bonora, S. Patergnani, A. Rimessi, E. D. Marchi, J. M. Suski, A. Bononi, C. Giorgi, S. Marchi, S. Missiroli, F. Poletti, M. R. Wieckowski, P. Pinton, ATP synthesis and storage. *Purinergic Signal.* **8**, 343–357 (2012).
49. J. J. Miller, *In vitro* experiments concerning the state of polyphosphate in the yeast vacuole. *Can J Microbiol.* **30**, 236–246 (1984).
50. F. Beaufay, E. Quarles, A. Franz, O. Katamanin, W.-Y. Wholey, U. Jakob, Polyphosphate functions *in vivo* as an iron chelator and Fenton reaction inhibitor. *mBio.* **11**, e01017-20 (2020).
51. R. Lr, T. Ei, D. Mg, S. Mc, J. Gj, N. Dk, Polyphosphate granule biogenesis is temporally and functionally tied to cell cycle exit during starvation in *Pseudomonas aeruginosa*. *Proc Natl Acad Sci U S A.* **114** (2017), doi:10.1073/pnas.1615575114.
52. S. Eixler, U. Selig, U. Karsten, Extraction and detection methods for polyphosphate storage in autotrophic planktonic organisms. *Hydrobiologia.* **533**, 135–143 (2005).
53. Y. Yu, L. You, D. Liu, W. Hollinshead, Y. J. Tang, F. Zhang, Development of *Synechocystis* sp. PCC 6803 as a phototrophic cell factory. *Mar Drugs.* **11**, 2894–2916 (2013).